Exploring temporal and spatial variation of nitrous oxide flux using several years of peatland forest automatic chamber data

Helena Rautakoski[1], Mika Korkiakoski[1], Jarmo Mäkelä[2], Markku Koskinen[3], Kari Minkkinen[4], Mika Aurela[1], Paavo Ojanen[4,5], Annalea Lohila[1,6]

[1]Finnish Meteorological Institute, P.O. Box 503, FI-00101 Helsinki, Finland
[2]Advanced Computing Facility, CSC – IT Center for Science Ltd, P.O. Box 405, FI-02101 Espoo, Finland
[3]Department of Agriculture, University of Helsinki, Viikinkaari 9, FI-00790 Helsinki, Finland
[4]Department of Forest Sciences, University of Helsinki, P.O. Box 27, FI-00014 Helsinki, Finland
[5]Natural Resources Institute Finland, Viikinkaari 4, FI-00790 Helsinki, Finland
[6]Institute for Atmospheric and Earth System Research, University of Helsinki, Gustaf Hällströmin katu 2, P.O. Box 64, FI-00014 Helsinki, Finland

Correspondence to: Helena Rautakoski (helena.rautakoski@fmi.fi)

Abstract: The urgent need to mitigate climate change has evoked a broad interest in better understanding and estimating nitrous oxide (N_2O) emissions from different ecosystems. Part of the uncertainty in N_2O emission estimates still comes from an inadequate understanding of the temporal and small-scale spatial variability of N_2O fluxes. Using 4.5 years of N_2O flux data collected in a drained peatland forest with six automated chambers, we explored temporal and small-scale spatial variability of N_2O fluxes. A Random forest with conditional inference trees was used to find immediate and delayed relationships between N_2O flux and environmental conditions across seasons and years.

The spatio-temporal variation of the N_2O flux was large, with daily mean N_2O flux varying between –10 and +1760 µg N_2O m^{-2} h^{-1} and annual N_2O budgets of different chambers between +60 and +2110 mg N_2O m^{-2} y^{-1}. Spatial differences in fluxes persisted through years of different environmental conditions. Soil moisture, WTL and air temperature were the most important variables explaining the temporal variation of N_2O fluxes. N_2O fluxes responded to precipitation events with peak fluxes measured on average 4 days after peaks in soil moisture and water table level. The length of the time lags varied in space and between seasons indicating possible interactions with temperature and other soil conditions.

The high temporal variation in N_2O flux was related to a) temporal variation in environmental conditions, with the highest N_2O fluxes measured after summer precipitation events and winter soil freezing, and b) to annually varying seasonal weather conditions, with the highest N_2O emissions measured during wet summers and winters with discontinuous snow cover. Climate change may thus increase winter N_2O emissions, which may be offset by lower summer N_2O emissions in dry years. The high sensitivity of N_2O fluxes to seasonal weather conditions suggests increasing variability in annual peatland forest N_2O budgets as the frequency of extreme weather events, such as droughts, is predicted to increase.

1. Introduction

Among the greenhouse gases whose emissions contribute to climate change, nitrous oxide (N_2O) is one of the most potent, with a 100-year global warming potential 273 times greater than that of carbon dioxide (Forster et al., 2021). A major part of N_2O emissions originates from soils (Butterbach-Bahl et al., 2013; Davidson and Kanter, 2014). Human impact through altered nitrogen (N) cycling, land use and climate change affect the soil N_2O emissions in both natural and managed ecosystems (Tian et al., 2018, 2020). The urgent need to mitigate climate change has evoked a broad interest in better understanding and estimating N_2O emissions of different ecosystems (Thompson et al., 2019; Shakoor et al., 2021). However, the accurate estimation of N_2O emissions has remained a challenge and emissions estimates continue to have relatively high uncertainties (Tian et al., 2020). A large part of the uncertainty in N_2O emission estimates is due to inadequate understanding of the temporal and small-scale spatial variability of N_2O fluxes (Sutton et al., 2007; Groffman et al., 2009; Kuzyakov and Blagodatskaya, 2015; Wang et al., 2020).

N_2O is formed in multiple processes, each favored by different soil conditions (Butterbach-Bahl et al., 2013). The main processes producing N_2O in soils are nitrification and denitrification (Bollmann and Conrad, 1998; Zhu et al., 2013; Hu et al., 2015). Nitrifying bacteria turn ammonium into nitrate in aerobic conditions. Nitrate produced in nitrification can further be reduced to nitric oxide, N_2O and gaseous nitrogen (N_2) in oxygen-limited or anaerobic conditions (Wrage et al., 2001; Zhu et al., 2013; Wrage-Mönnig et al., 2018), making the availability of oxygen a key control of N_2O flux (Song et al., 2019). Oxygen limitation in soil and substrate availability for microbes is affected by soil water content, which makes N_2O production also sensitive to varying soil moisture conditions (Butterbach-Bahl et al., 2013). Along with soil moisture, substrate availability is widely affected by human actions, such as fertilization, nitrogen deposition and drainage of organic soils, which are all linked to increased N_2O fluxes (Pärn et al., 2018; Tian et al., 2020; Lin et al., 2022). Soil temperature regulates microbial activity in the soil, but it also shapes microbial community composition and affects N_2O production through, for example, frost, ice formation and thaw (Holtan-Hartwig et al., 2002; Risk et al., 2013; Wagner-Riddle et al., 2017).

Temporal variation of soil conditions can lead to a high temporal variation of N_2O flux within a year (Groffman et al., 2009; Kuzyakov and Blagodatskaya, 2015). Soil freeze-thaw and dry-wet cycles are examples of changes in soil conditions shown to shape seasonal variation in N_2O emissions (Risk et al., 2013; Congreves et al., 2018). High temporal variation of N_2O flux has been shown to be typical for several ecosystems (Luo et al., 2012; Molodovskaya et al., 2012; Anthony and Silver et al., 2021), but understanding related to the temporal variation of N_2O production is limited by sparse sampling intervals of manual flux measurements, lack of short-interval measurements and poor temporal coverage of data from all parts of the year (Barton et al., 2015; Grace et al., 2020). Since short periods of high N_2O fluxes can account for a substantial amount of the annual N_2O budget (Molodovskaya et al., 2012; Ju and Zhang, 2017; Anthony and Silver, 2021), capturing N_2O flux peaks and understanding the causes of temporal variation of N_2O flux are essential for estimating annual emissions accurately.

High spatial variation is also typical for N_2O flux and occurs on multiple spatial scales from large-scale variation between ecosystems to small-scale variation within a few meters (Groffman et al., 2009; Krichels and Yang, 2019). High N_2O fluxes are typically measured in ecosystems with high N availability, such as in agricultural fields and in drained organic soils where fertilization and organic matter mineralization provide N supply for N_2O production

(Maljanen et al., 2003; Reay et al., 2012; Leppelt et al., 2014; Pärn et al., 2018). Within an ecosystem, varying soil properties and conditions such as organic matter content, soil moisture or pH can create spatial variability in the N_2O fluxes (Jungkunst et al., 2012; Giltrap et al., 2014). Although the small-scale spatial variation of N_2O flux can be large and exceed the spatial variation between more distant parts of the same ecosystem (Yanai et al., 2003; Jungkunst et al., 2012; Giltrap et al., 2014), the causes of small-scale spatial variability of N_2O flux are poorly known and little studied, especially with short-interval measurements. Several questions related, for example, to the persistence of spatial patterns over time and linkages between the spatial and temporal variation of N_2O flux are little understood.

Drained peatland forests are examples of ecosystems with relatively high N_2O fluxes and high spatio-temporal variation of those fluxes (Maljanen et al., 2003; Minkkinen et al., 2020; Pärn et al., 2018). In Finland, about 60 % of the original peatland area has been drained for forestry (Korhonen et al., 2021), which has resulted in a lowered groundwater level and increased N availability for N_2O production from the decomposing peat. Drainage has led to increased N_2O fluxes, especially in nutrient-rich peatland forests with a low C:N ratio (Martikainen et al., 1993; Laine et al., 1996; Klemedtsson et al., 2005). The focus of previous studies on peatland forest N_2O fluxes has been mainly on understanding the large-scale spatial variation of N_2O fluxes between different peatland forests (Klemedtsson et al., 2005; Ojanen et al., 2010; Minkkinen et al., 2020) and reporting N_2O flux response to forest harvesting or other forestry operations (Maljanen et al., 2003; Huttunen et al., 2003; Korkiakoski et al., 2019, 2020). Temporal variation has been mainly studied with sparce-interval chamber measurements (Maljanen et al., 2010; Pihlatie et al., 2010).

For the first time in boreal drained peat soils, we use multiple years (2015–2019) of automated chamber N_2O fluxes to investigate the characteristics of temporal and small-scale spatial variation in N_2O flux. We link the temporal variation of N_2O flux to seasonally and annually variable environmental conditions including immediate and time-lagged responses. This is done to provide a more comprehensive understanding of the spatio-temporal dynamics of N_2O flux and to reduce uncertainties in current and future N_2O emission estimates in boreal peatland forests and beyond.

2. Materials and methods

2.1. Site description

The flux measurements were conducted between the 1st of June, 2015 and 29th of September, 2019 in a drained nutrient-rich peatland forest located in southern Finland (Lettosuo, 60°38′ N, 23°57′ E). The mean annual temperature in the area is 5.2 °C and the mean annual precipitation 621 mm according to the long-term weather record from the nearest automatic weather station (Jokioinen Ilmala, 1991–2020, 35 km from the study site). The site was initially drained in the 1930s and more intensively in 1969 to promote tree growth. Ditches were dug about 1 m deep and 45 m apart. The site was fertilized with phosphorus and potassium after the later drainage. Drainage lowered the groundwater table, resulting in a transition to boreal-forest-like vegetation. The relatively low C:N ratio reflects the fen history of the site (Table 1).

Before March 2016, the site was a mixed forest with an overstory dominated by Scots pine (*Pinus sylvestris*) and an understory dominated by Norway spruce (*Picea abies*). Both overstory and understory contained a small

amount of downy birch (*Betula pubescens*). Overstory pines were removed during a selection harvest in March 2016 (70 % of the total stem volume; Korkiakoski et al., 2020, 2023). The surroundings of the measurement chambers used in this study were harvested more lightly, and the chamber area continued to have a high coverage of spruce and birch. The selection harvest did not affect N_2O fluxes according to the previous study from the site (Korkiakoski et al., 2020), and the effect of the harvest was left out of the focus of this study.

Table 1: Soil properties at the study site. Values represent general soil properties at the study site before the selection harvest was done. Data from Korkiakoski et al. (2019).

Depth	Total-N (%)	Total-C (%)	C:N	Bulk density (g cm^{-3})
Humus	1.7 ± 0.4	56.2 ± 2.3	33.2 ± 2.3	0.01 ± 0.003
0–10 cm	2.2 ± 0.2	55.2 ± 2.1	24.9 ± 2.1	0.12 ± 0.03
10–20 cm	2.5 ± 0.2	58.9 ± 1.6	23.8 ± 1.6	0.18 ± 0.02

2.2. Automatic chamber fluxes

The N_2O flux between the forest floor and the atmosphere was measured using six automated chambers. The transparent, acrylic, rectangular cuboid chambers with the dimensions 57 x 57 x 40 cm (length x width x height) were placed to sample the spatial variation of the ground vegetation composition within an area of 15 x 20 m (Fig. 1). The chambers were placed on permanently installed steel collars that were inserted into the soil to a depth of 2 cm. All the chambers closed for six minutes once an hour year-round. The chambers had an air temperature sensor and a fan to mix the air inside the chamber headspace. During winters, chambers were cleaned from snow and ice every 1–3 weeks and snow depth inside the chambers was measured to account for the effect of snow depth on chamber volume. During the winter 2016–2017, extension collars were used to better allow snow to fit inside the chambers.

The N_2O concentration of the chamber headspace air was measured using a continuous wave quantum cascade laser absorption spectrometer (LGR-CW-QCL N_2O/CO-23d, Los Gatos Research Inc., Mountain View, CA, USA) that was placed in a measurement cabin close to the chambers (Fig. 1b). The analyzer had an accuracy of 0.01 ppb per second, corresponding to a minimum detectable flux (Nickerson, 2016) of 0.06 µg N_2O m^{-2} h^{-1} in our chamber system. During each chamber closure, air from the closed chamber was pumped into the analyzer and back to the chamber headspace through plastic tubes (length 15 m, flow about 1 l/min). After each chamber closure, the airflow was switched to the next chamber. Ambient air was measured for at least 1 min between the chamber closures to allow concentrations in the tubes to stabilize back to the ambient level. Concentration data from the first 30 s of each chamber closure were not used in flux calculation to avoid possible pressure disturbance caused by the closing chamber affecting the flux (Pavelka et al., 2018). For more information about the automatic chamber system, see the previous studies from the same site (Koskinen et al., 2014; Korkiakoski et al., 2017, 2020). Measurements in Chamber 6 ended six months earlier (April 2019) than measurements in other chambers due to problems in chamber functioning.

N_2O fluxes were calculated similarly to Korkiakoski et al. (2017), but by using a linear fit. The mean headspace temperature of the closure and air pressure measured at the site were used in the flux calculation. Calculated fluxes were filtered using normalized root mean square error and an iterative standard deviation filter to remove

erroneous fluxes resulting from chamber malfunction (Korkiakoski et al., 2017). Daily mean N_2O fluxes from each chamber were used in the analysis because the automatic chamber system seemed to create an artificial diurnal cycle of N_2O from which the possible natural diurnal cycle could not be separated. The artificial diurnal cycle was caused by the difference in turbulence between the ambient air and chamber headspace, as previously reported for CO_2 and CH_4 (Koskinen et al., 2014; Korkiakoski et al., 2017). During calm periods, especially during summer nights, the transfer of N_2O from soil pores to the atmosphere slowed down, leading to increased N_2O concentration in the soil. When the chamber closed and the turbulence increased because of the fan, the N_2O from the soil pores was vented to the chamber headspace air, leading to overestimated flux. The opposite phenomenon probably occurred in windy conditions, resulting in underestimated flux. Based on our experience, automatic chamber fluxes measured in drained peatlands with dry and porous peat soil are particularly sensitive to this phenomenon (Koskinen et al., 2014; Korkiakoski et al., 2017). Hourly N_2O flux peaks were not typical in the flux data, and daily mean N_2O fluxes thus well represent the main characteristics of the temporal variation. It should be noted that the artificial diurnal cycle creates an additional source of uncertainty in the reported N_2O budgets.

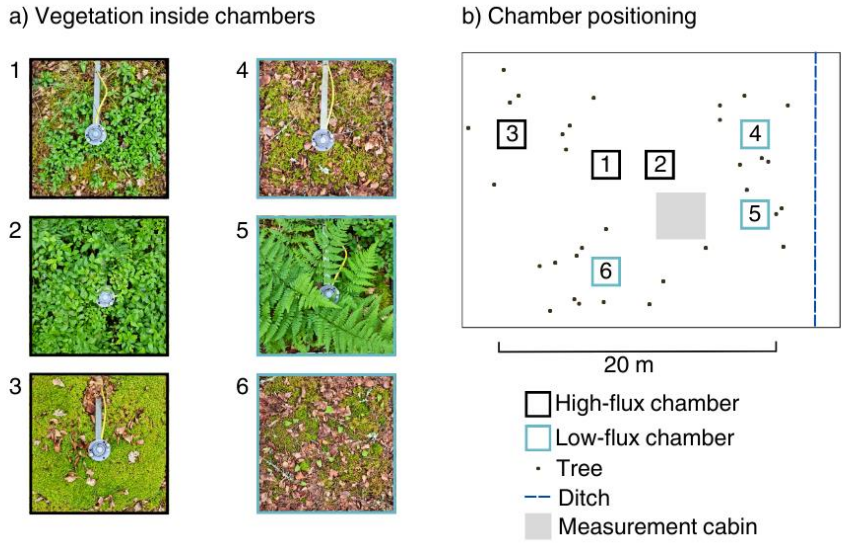

Figure 1: (a) Vegetation inside the six chambers and (b) the positioning of the chambers on the forest floor in relation to the nearest ditch and trees. Chambers are named from one to six based on the maximum measured flux with Chamber 1 having the highest measured flux. Chambers 1–3 with black edges are classified as "high-flux chambers" and Chambers 4–6 with blue edges as "low-flux chambers". For more information on chamber vegetation, ditches and trees, see Table S1.

2.3. Environmental variables

Several environmental variables were measured to link the temporal variation of N_2O fluxes with the environmental conditions. Air temperature was measured at 2 m height below the forest canopy (HMP45D, Vaisala Oyj, Vantaa, Finland). Soil surface temperature was measured at 2 cm depth in each chamber and the soil temperature at 5 cm depth at one location close to the chambers (Pt100, Nokeval Oy, Nokia, Finland). Soil moisture was measured at one location about 75 m from the chamber measurement location at 7 and 20 cm depths (Delta-T ML3, Delta-T Devices Ltd, Cambridge, UK). The soil moisture data were used to describe the temporal variation of soil moisture,

assuming that the soil moisture had relatively similar temporal patterns across the study site. The absolute level of soil moisture in each chamber may have differed from the measured soil moisture, and the possibility of differences in the temporal variation of soil moisture between the logger and the chambers cannot be excluded. Soil moisture data were used together with water table level and precipitation data to strengthen the conclusions related to soil water conditions. The measurements of air and soil temperatures were ongoing throughout the study period, but the soil moisture measurements ended half a year earlier than automatic chamber measurements (April 2019).

Water table level (WTL) below the soil surface was measured using automatic loggers (TruTrack WT-HR, Intech Instruments Ltd, Auckland, New Zealand; Odyssey Capacitance Water Level Logger, Dataflow Systems Ltd, Christchurch, New Zealand). Chambers 1–2 and 4–5 shared a WTL logger that was placed between the chamber pairs. Chambers 3 and 6 had WTL loggers next to the chambers. WTL measurements for Chambers 3–6 started half a year later than chamber measurements (December 2015). WTL during this and other data gaps was modeled using random forest with conditional inference trees (Hothorn et al., 2006). WTL data from Chambers 1–2, seven other WTL loggers at the study site and precipitation were used as explanatory variables in the gap-filling model. Modeling was done first for the logger with the least amount of missing data, after which the gap-filled WTL time series was added to the model as an explanatory variable to increase the predictive power of the model for the variables with more missing data (evaluation data R^2 = 0.90–0.97).

Precipitation was measured at the site throughout the study period (Casella Tipping Bucket Rain Gauge, Casella Solutions Ltd, Bedford, UK; OTT Pluvio2 L 400 RH, OTT Hydromet Ltd, Kempten, Germany) and daily precipitation sum was calculated. The precipitation data measured at the nearest weather station was used to gap-fill winters and other measurement gaps in precipitation data (correlation of precipitation between sites 0.65, $p < 0.05$). Snow depth measured at the nearest weather station was used to describe general snow conditions experienced each winter. Thermal seasons were used to analyze the seasonality of N_2O fluxes. The thermal seasons were defined according to typical Finnish standards (Ruosteenoja et al., 2016; Finnish Meteorological Institute, 2023) by using air temperature data from the site (Appendix A). Seasons based on months were used to compare conditions measured at the site with long-term averages reported monthly for the nearest weather station.

2.4. Identifying high-flux periods

The term “high-flux period” was used to describe periods of elevated flux, including periods from moderately increased flux to the highest flux peaks. ”High-flux period” was used instead of a commonly used “hot moment” because the definition of a hot moment largely varies between studies, with sometimes only extremely high fluxes being considered as hot moments (Molodovskaya, 2012; Krichels and Yang, 2019; Anthony and Silver, 2021; Song et al., 2022).

To identify the high-flux periods, their length, seasonality and starting conditions, different thresholds to separate high-flux days from the baseline days were tested. High fluxes were measured less frequently compared to the more common low fluxes (Fig. S2). Any percentile threshold between 60–80 % separated high-flux days from the more common baseline fluxes relatively well, and the mean of these (70 %) was used. Days with the mean flux above the 70 % percentile were classified as high-flux days and the rest of the days as baseline days. The length of each

high-flux period was the number of days the flux remained above the 70 % percentile, including possible data gaps within this period. The high-flux period was set to continue over a data gap if three days before and after the data gap were classified as high-flux days. A three-day marginal was chosen to ensure that short one-to-two-day peaks would not create long-lasting high-flux periods over data gaps. If the high-flux period started from a data gap or ended to it, the start or end date of the high-flux period was set to the first or last measured day, respectively. Pearson correlation was used to test how similar the temporal patterns of N_2O flux were between chambers.

2.5. Machine learning

Machine learning models were used to improve understanding of the temporal controls on N_2O flux, including a possible effect of time lags between environmental conditions and N_2O flux. The machine learning approach was used because machine learning models do not rely on mathematical functions to describe relationships between variables and are able to account for interactions between variables flexibly (Olden et al., 2008). The Random forest algorithm, developed by Breiman (2001), is a classification tree-based method that uses bootstrap aggregation of a model training data and a randomly chosen subset of explanatory variables (*mtry*-parameter) to train each classification tree. In bootstrap aggregation, a subset of data is taken from the model training data with or without returning it to the original training data. The part of data that is not bootstrapped to train trees is called out-of-bag (OOB) data and it can be used to evaluate model performance. In each random forest tree, the bootstrapped data are classified into subgroups and further into smaller subgroups by setting threshold values for the randomly chosen subset of explanatory variables. The setting of the threshold values is done to maximize the information gain until no further thresholds, also called splits, can be made. After a selected number of trees are built, the final model prediction can be made using the average of all the trees (continuous response) or the most common outcome (categorical response).

Random forest variable importance (VI) metrics show the importance of each explanatory variable in explaining variation in the response variable. VI metrics can be biased if the explanatory variables correlate (Strobl et al., 2007). Therefore, we used random forest with conditional inference trees (Hothorn et al., 2006) that allowed us to get more accurate VIs in the presence of correlated explanatory variables and their time-lagged versions. Compared to trees in random forest, conditional inference trees use a p-value-based splitting criterion to classify the bootstrap aggregated data in the building phase of each tree. As suggested by Strobl et al. (2007), in the presence of correlated explanatory variables, variable importance metrics from the conditional inference trees were calculated using conditional permutation importance.

Chamber-specific models had daily mean N_2O flux as the response variable and the measured temperature variables (air, soil 2 cm and 5 cm depths), soil moisture (7 and 20 cm depths), WTL and daily cumulative precipitation as explanatory variables. Periods of missing data in environmental variables were gap-filled using the random forest proximity tool RFimpute (Liaw and Wiener, 2002). One-to-seven days' time-lagged versions of each environmental variable were added as explanatory variables to the models besides unlagged environmental variables. The imbalanced distributions of N_2O fluxes were corrected with the SMOGN algorithm (Abd Elrahman and Abraham, 2013). The subset of data to train each tree was bootstrapped without replacement with a sample size 0.632 times the size of the

training dataset, as suggested by Strobl (2007). Models were trained with 500 trees and random forest default *mtry* for continuous response variable was used (*mtry* = number of explanatory variables / 3).

The first three years of data were utilized as the model training period (June 2015 – June 2018), and this data were further split into 70 % training data and 30 % evaluation data to test model performance within the training period. The fourth year of measurements until soil moisture measurements ended (June 2018 – April 2019) was left aside for evaluation to test model performance outside the training period. The performance of the models on different evaluation datasets was analyzed using R squared (R^2) and root mean squared error (RMSE). R^2 was used to compare model performance between chambers. Variable selection was not done. Evaluation results are presented in appendices (Appendix B).

VIs and accumulated local effects (ALE) were used to interpret the modeling results. For easier comparison of VIs across chambers, the VIs of each chamber were scaled from zero to one (0 = least important variable, 1 = most important variable) and the total VIs of each variable were calculated (total VI = VI of unlagged variable + VIs of lags). The ALE method by Apley and Zhu (2020) was used to visualize the response of N_2O flux to environmental conditions and their lags in the models. In ALE figures, ALE value (y-axis) zero refers to the mean predicted N_2O flux, with a positive ALE value meaning larger and a negative value lower predicted N_2O flux in a specific environmental condition (x-axis). ALE values for lagged environmental variables indicate the response of predicted N_2O flux to previous environmental conditions. From the unlagged and lagged versions of each environmental variable, the one that received the highest ALE value for a given environmental condition was considered to represent the typical response time of N_2O flux to that condition. In this article, the response time, or lag length in the presence of at least a one-day lag, refers to the time it takes for N_2O to reach peak flux after the onset of a given environmental condition. The reported evaluation results (RMSE, R^2), VIs, and ALE values are averages over 10 model runs.

2.6. N_2O budgets

Data gaps covered 12–24 % of the study period depending on the chamber. Daily mean N_2O flux time series were gap-filled to calculate N_2O budgets. Gap-filled data were not used in other analyses to avoid additional uncertainty arising from the gap-filling. The same models and explanatory variables were used as in the machine learning part, including time-lagged variables. The fourth measurement year previously left for evaluation was also included in the training data for gap-filling. To test the performance of the gap-filling model, separate models were run with 70 % and 30 % split to the training data and evaluation data, respectively. Evaluation metrics (RMSE, R^2) of gap-filling models are shown in Appendices (Appendix B). Gap-filled daily mean N_2O fluxes were used to calculate N_2O budgets for each chamber in each thermal season. The uncertainty related to the N_2O budgets was assumed to be a combination of uncertainty related to flux measurement and uncertainty related to gap-filling. Detailed information about the calculation of the uncertainty can be found in Korkiakoski et al. (2017).

Flux calculation was performed in the Python programming language version 2.7 (Van Rossum and Drake, 1995). Data preparation and analysis were performed in R statistical software version 4.0.5 (R core team, 2021). Cforest-command in the party package (Hothorn et al., 2006; Strobl et al., 2007; Zeileis et al., 2008) was used to

perform random forest with conditional inference trees. Data and simplified R-code about the machine learning part of the study are made freely available (See Sect. 7).

3. Results

3.1. Environmental conditions

The summers (June, July, August) 2015 and 2017 were colder (seasonal means 14.1 °C and 14.4 °C, respectively) than the long-term average (15.6 °C, Jokioinen-Ilmala 1991–2020), and winters (December, January, February) 2015–2016, 2016–2017 and 2018–2019 were warmer (seasonal means –3.4 °C, –3.0 °C and –3.5 °C, respectively) than the long-term average (–4.3 °C) (Fig. 2). Temperatures were warm in all seasons in 2018 and 2019, with the summer (seasonal mean 17.2 °C) and autumn (seasonal mean 6.7 °C) 2018 being particularly warm compared to the long-term averages (summer 15.6 °C and autumn 5.4 °C). The area received the least amount of precipitation in 2018 (annual sum 434 mm) and the most precipitation in 2017 (annual sum 657 mm) with the long-term annual average being 621 mm. The summer 2018 (seasonal sum 44 mm) was especially dry compared to the long-term average summer precipitation of 71 mm. The drought that began in the spring 2018 continued until autumn.

Soil moisture was continuously lower than the mean of the study period from the summer 2018 until the end of the study period (Fig. 3), with the study period mean being 0.28 m^{-3} m^{-3} for 7 cm soil moisture and 0.56 m^{-3} m^{-3} for 20 cm soil moisture. WTL was on average –36 cm and continuously deeper than that in the summer and autumn 2015 as well as in the summers 2018 and 2019. Soil temperatures at 5 cm depth reached freezing temperatures in winters 2015–2016 (min. –3.8 °C), 2016 –2017 (min. –1.8 °C) and 2017–2018 (min. –0.33 °C). Variation of air and soil surface temperatures was high in winters 2015–2016 and 2016–2017. The snow cover was thickest in winter 2018–2019 (max. 52 cm) and thinnest in winter 2016–2017 (max. 11 cm). The number of days with snow cover was lower in winters 2015–2016 (85 days) and 2016–2017 (93 days), and higher in winters 2017–2018 (125 days) and 2018–2019 (116 days).

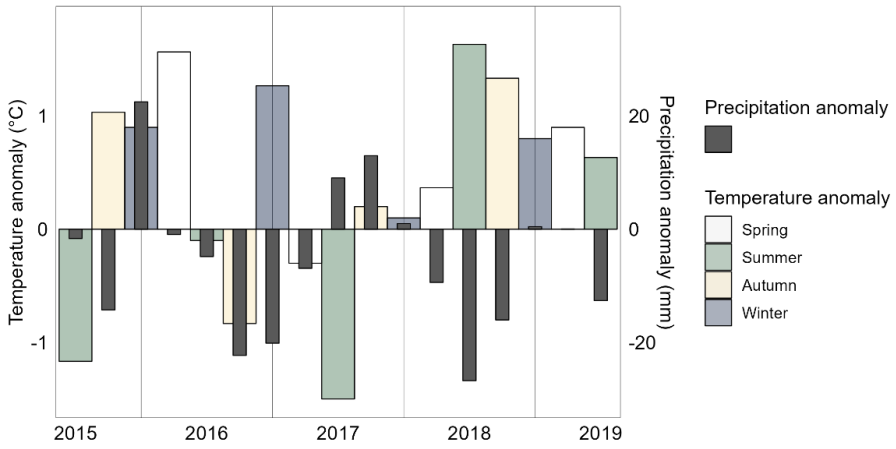

Figure 2: Difference of seasonal mean air temperature and precipitation sum from the long-term average. The long-term averages from the nearest weather station are used (Jokioinen Ilmala, 1991–2020). Seasons are based on months (autumn: September–November, winter: December–February, spring: March–May and summer: June–August).

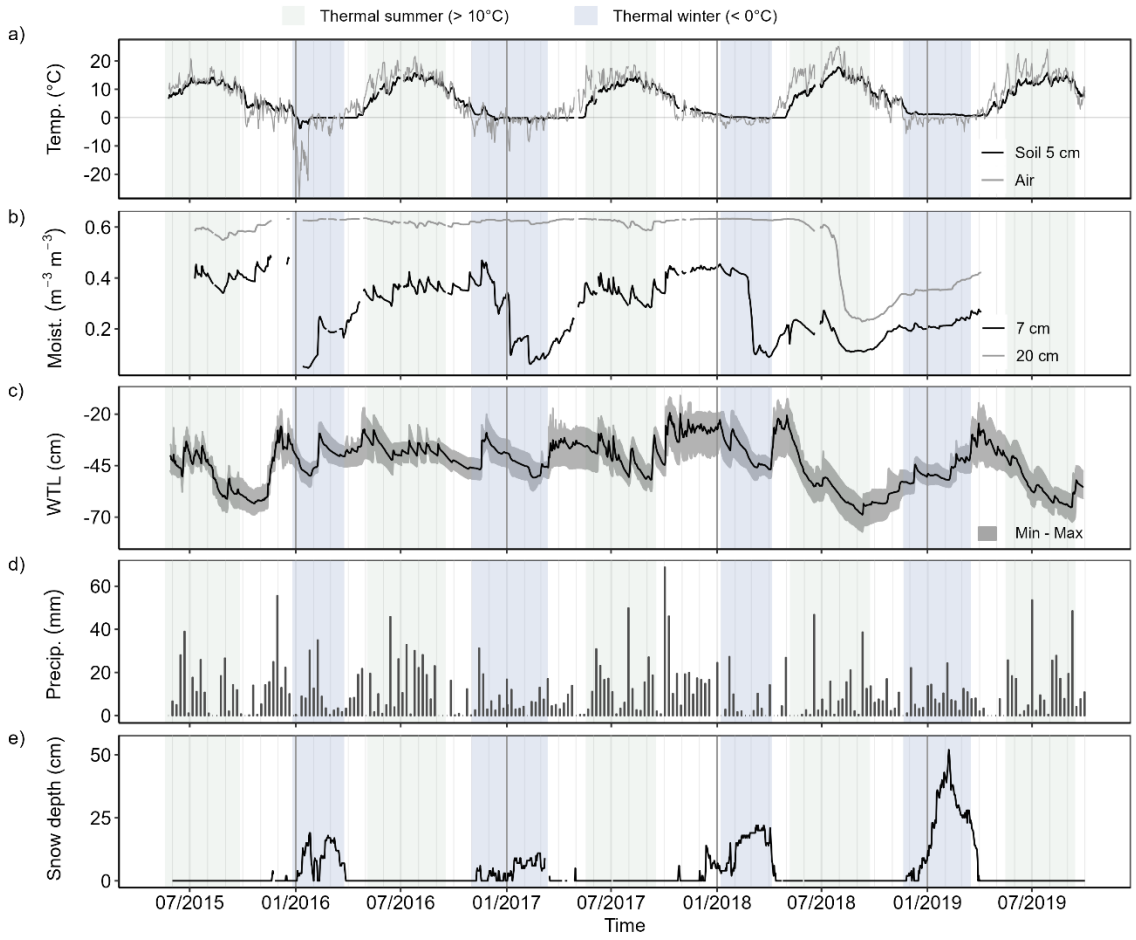

Figure 3: (a) Daily mean air and soil temperatures (5 cm depth), (b) soil moisture (7 and 20 cm depths), (c) water table level (WTL), (d) weekly precipitation sum and (e) daily mean snow depth. WTL is the mean of the chambers with gray shading showing the range of WTL between different chambers. Snow depth was measured at the nearest weather station. Data are not gap-filled.

3.2. Temporal and spatial variation of N_2O flux

The daily mean N_2O flux varied between –10 and +1760 µg N_2O m^{-2} h^{-1} during the 4.5 years of measurements (Fig. 4). Three chambers (Chambers 1, 2 and 3) had maximum daily mean fluxes greater than 1100 µg N_2O m^{-2} h^{-1}, and the other three chambers (Chambers 4, 5 and 6) had maximum daily mean fluxes less than 400 µg N_2O m^{-2} h^{-1} (Table 2). Chambers 1–3 also had a higher mean flux than Chambers 4–6 in all years (Table S3.1). The annual mean flux was the highest in 2016 or 2017, depending on the chamber, and lowest in 2018 or 2019. Based on the differences in the maximum flux, standard deviation and the range of the flux variation, Chambers 1–3 were classified as "high-flux chambers" and Chambers 4–6 as "low-flux chambers".

The chamber-specific 70 % percentiles that were used to define the high-flux periods from the baseline periods ranged from 20 (Chamber 5 and 6) to 170 µg N_2O m^{-2} h^{-1} (Chamber 1, Table 2). The length of the individual baseline periods varied from 1 to 330 days with a mean of 26 days, while the length of the high-flux periods varied

between 1 and 134 days with the mean of 11 days. The correlation of flux time series between chambers varied between 0.79 (Chambers 1 and 2) and 0.29 (Chambers 1 and 4) (Table S4). Correlation was the highest between the chambers with a similar range of N_2O flux: among high-flux chambers, correlation varied between 0.64–0.79 and among low-flux chambers, between 0.46–0.49. Differences in WTL between chambers were statistically significant but were not associated with the spatial variation of N_2O flux.

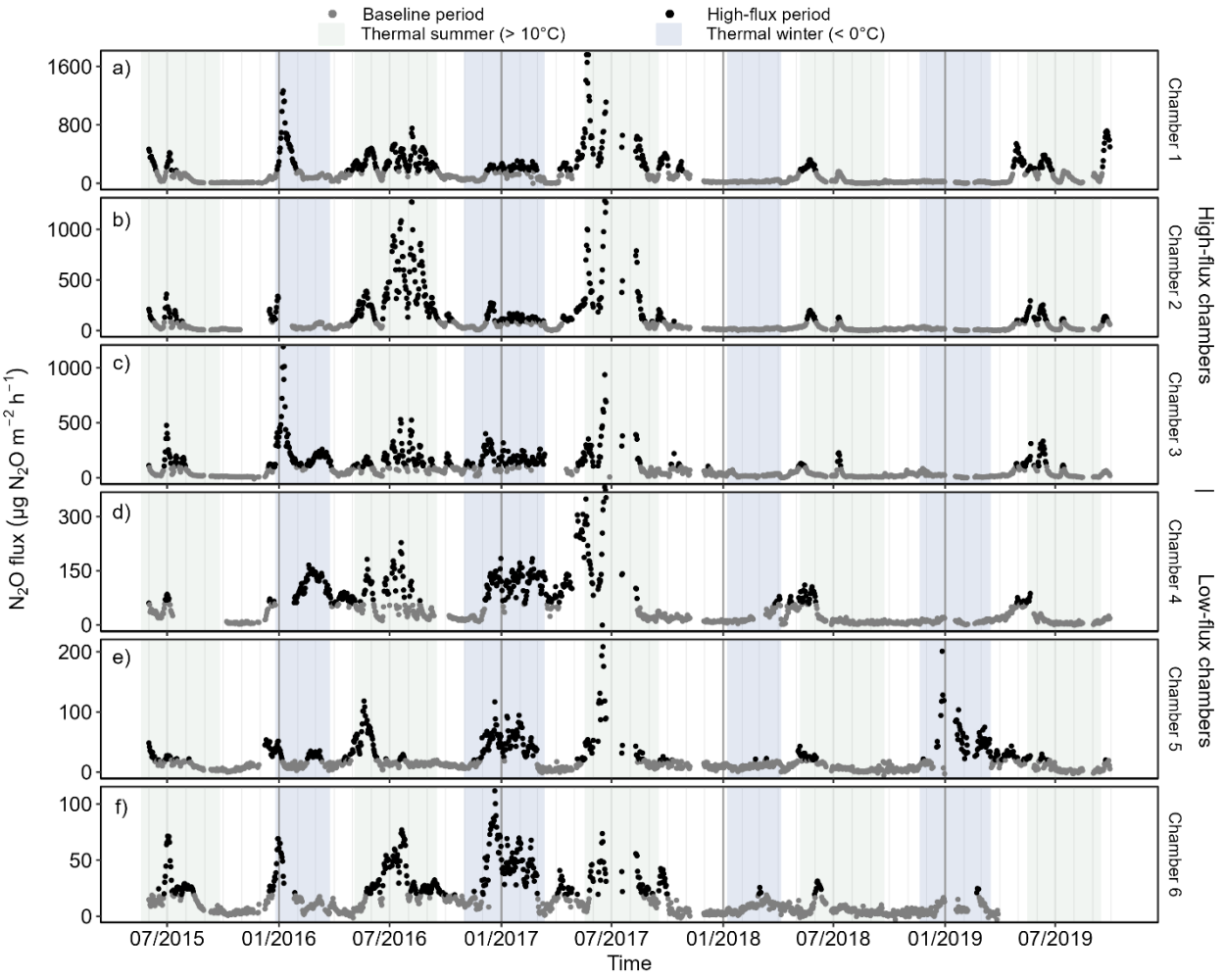

Figure 4: Daily mean N_2O flux measured in the six automatic chambers in 2015–2019. Fluxes from different chambers are shown in panels (a–f) ordered by maximum daily mean N_2O flux. Chambers are grouped into high-flux (Chambers 1, 2 and 3) and low-flux chambers (Chambers 4, 5 and 6). The scale of the y-axis is chamber specific and fluxes are not gap-filled. Periods with the daily mean fluxes > 70 % percentile are classified as high-flux periods.

Table 2: Minimum, maximum, mean, median, 70 % percentile and standard deviation (SD) of daily mean N_2O fluxes over the study period. The unit of the flux is µg N_2O m^{-2} h^{-1}. Percentile thresholds (70 %) were used to define high-flux periods. Year-specific statistics can be found in Table S3.1.

Source	Min	Max	Mean	Median	Percentile 70 %	SD
Chamber 1	–1	1761	143	73	168	193

Chamber 2	–1	1282	99	34	88	171
Chamber 3	–12	1192	87	46	100	112
Chamber 4	–1	381	48	22	58	57
Chamber 5	–5	244	20	13	20	23
Chamber 6	–3	112	17	11	19	17

3.3. Seasonality of N_2O flux

The highest N_2O fluxes were measured during thermal summers (Chambers 1, 2, 4 and 5) or winters (Chambers 3 and 6). The fluxes were also on average the highest in summers and winters, and the lowest in autumns (Tables S3). The percentage of measurement days identified as high-flux days averaged 24 % in spring, 38 % in summer and 44 % in winter and 9 % in autumn (Fig. 5). The highest proportion of winter and summer high-flux days were measured in 2016 and 2017, and the lowest proportion in 2018.

In spring, N_2O fluxes increased steadily as soil surface temperatures increased above zero (Fig. 6 and S5), with most of the spring high-flux periods starting at soil surface temperatures 0–2 °C (Fig. 7). Spring N_2O fluxes increased steadily with increasing soil temperatures, and flux peaks were reached in late spring or early summer. Summer high-flux periods started after precipitation events at moist soil conditions (0.37–0.41 m^{-3} m^{-3}) and during relatively high WTL (–35 to –50 cm depth) (Fig. 7), but the peak fluxes were reached several days after the rain events. The starting conditions for soil moisture and WTL in the autumn high-flux periods were similar to those in summer, but the response to soil wetting was slower and fluxes were smaller.

Winter high-flux periods started on soil temperatures close to 0 °C (Fig. 7). In early winter, N_2O fluxes increased when soil surface temperatures decreased to near zero and below that, with further increase in flux measured if soil temperature also at 5 cm depth decreased below zero (Fig. 6 and S5). Later in the winter, increased N_2O fluxes were measured during periods of soil freezing or when soil temperatures increased towards or above zero. Freezing of the soil surface did not typically lead to high N_2O fluxes without temperatures being below zero also at 5 cm depth. The response to soil freezing, especially in the early winter, was stronger than the response to soil thawing in terms of duration of the high-flux periods and peak flux.

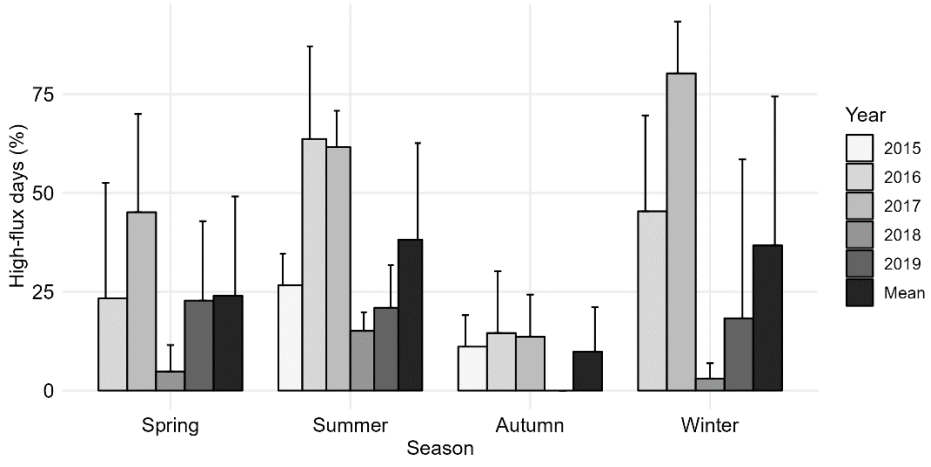

Figure 5: Occurrence of high-flux days out of measured days in different thermal seasons. Bars show annual means across different chambers and error bars show standard deviation between chambers. Mean bars show the mean across the years. The bar for winter 2019 only contains winter days between January – March 2019.

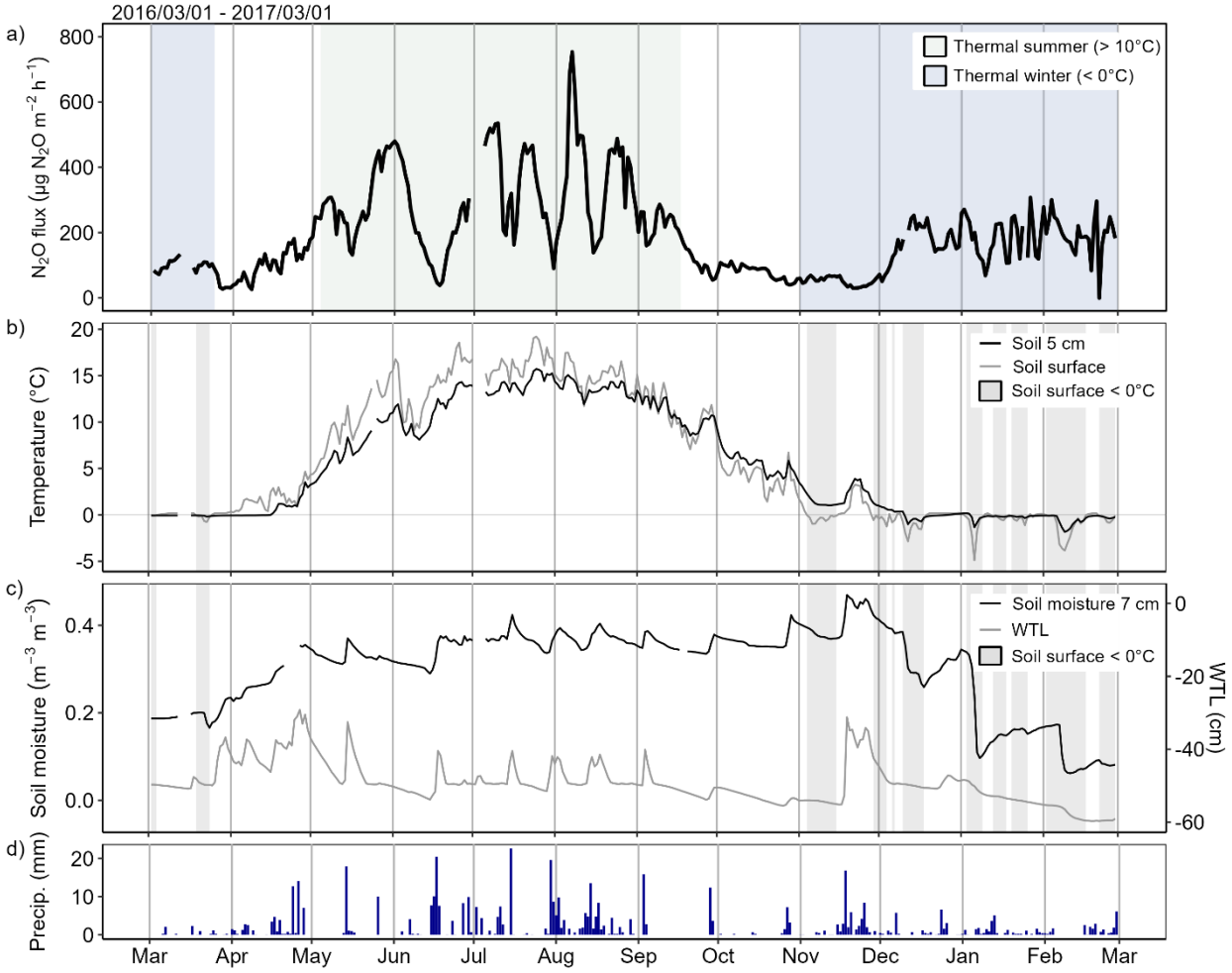

Figure 6: (a) Daily mean N_2O flux, (b) soil surface temperature and temperature at 5 cm depth with highlighted freezing periods (soil surface temperature < 0 °C), (c) soil moisture and water table level (WTL), and (d) daily precipitation from March 2016 to March 2017 in Chamber 1. The temporal variation of N_2O flux in Chamber 1 was similar to the other chambers, but the range of flux variation was larger compared to the low-flux chambers. The shown temporal dynamics of N_2O flux were measured in a year with relatively wet summer and warm winter. Data are not gap-filled. Figures for other chambers are presented in the supplements (S5).

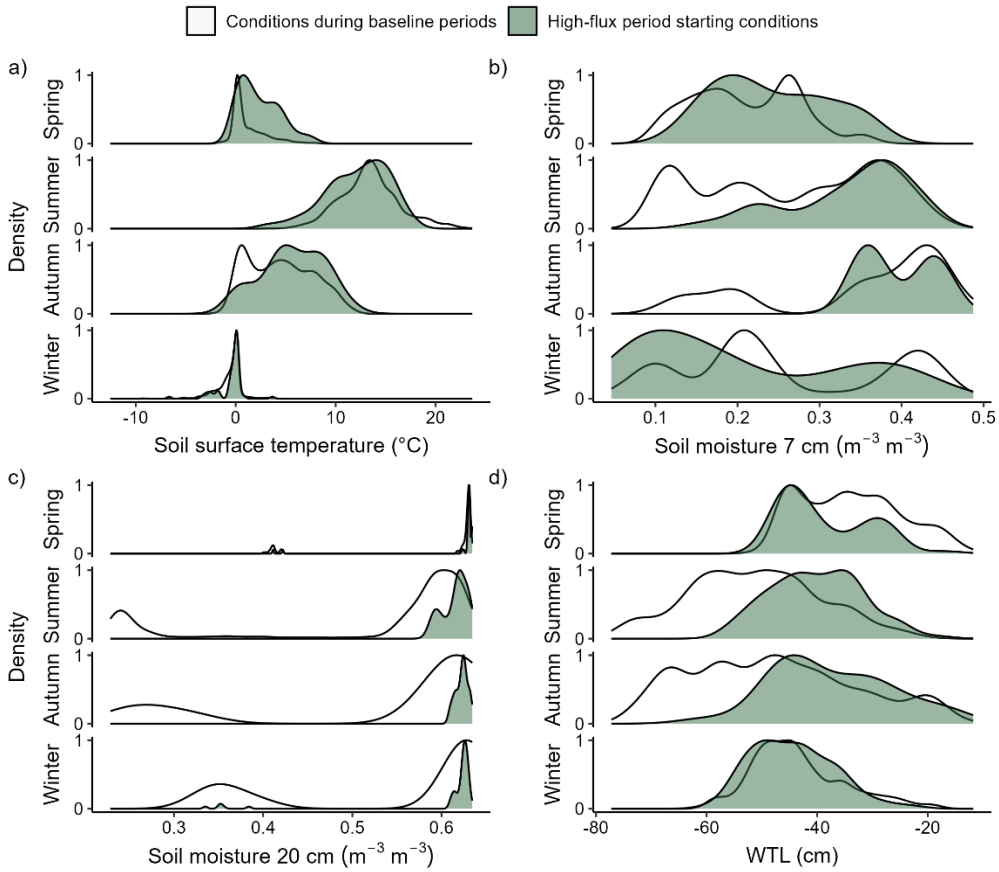

Figure 7: High-flux period starting conditions in each season compared to conditions outside the high-flux periods. Density plots show the distribution of high-flux periods starting on different (a) soil surface temperature, (b) soil moisture at 7 cm depth, (c) soil moisture at 20 cm depth, (d) and water table level (WTL). The Y-axis shows scaled (0–1) proportion (%) of high-flux periods starting on conditions shown on the x-axis (1=most common high-flux periods starting condition, 0=no starting high-flux periods). For comparison, the variation in soil conditions during baseline periods is also shown (1=most common baseline period condition, 0=no such condition measured during baseline periods). All years and chambers are included.

3.4. Machine learning

Soil moisture (both 7 and 20 cm), air temperature and WTL were considered to be the most important variables explaining the temporal variation of N_2O flux (Fig. 8) with the mean total variable importance (VI, 0 = no importance, 1 = high importance) being 0.7 and 0.6 for soil moisture (7 and 20 cm respectively) and 0.5 for air temperature and WTL. The mean VI of lags (1–7 days) for each environmental variable was the highest for 7 and 20 cm soil moisture (mean VI 0.3 for both) with 5 cm soil temperature and air temperature also having importance on lags (mean VI 0.25 and 0.20, respectively, Fig. S6). Lags of other variables received mean VIs lower than 0.1, but precipitation had an increasing VI towards the longest lags (6–7 days).

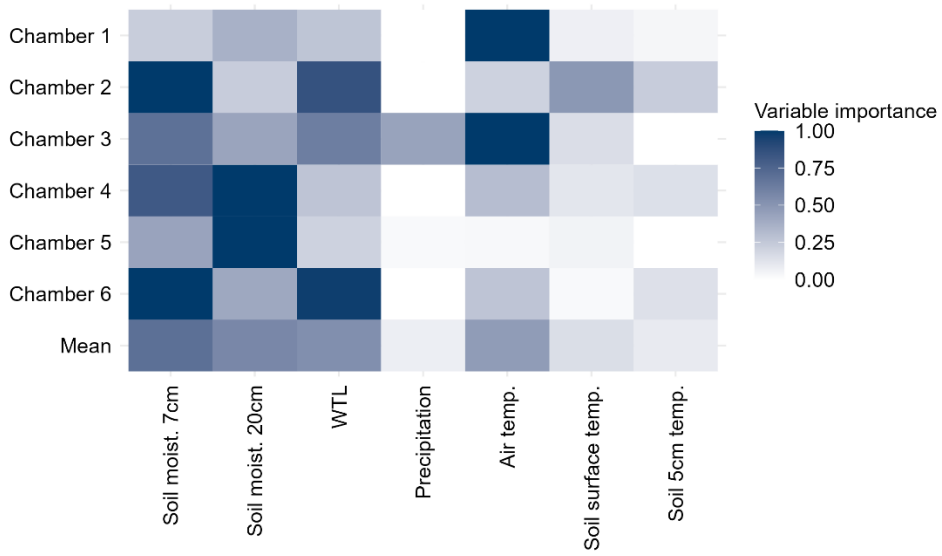

Figure 8: Total variable importance (VI) of different environmental variables in explaining the temporal variation of N_2O flux in random forest with conditional inference trees. Total VI is the sum of VIs of unlagged and lagged (1–7 days) versions of the variable. Rows in the matrix plot show VIs for different chambers and the mean VIs across all the chambers (Mean). VI scores are scaled between 0 and 1 (0 = no importance, 1 = highest importance) per chamber. Lag-specific VIs are shown in Fig. S6.

Accumulated local effects (ALE) for 7 cm soil moisture showed that the highest fluxes were predicted for the 1–7 days lagged soil moisture when the soil was moist (> 0.35 m^{-3} m^{-3}). The lag with the highest predicted flux varied from 1 to 7 days between chambers with a mean lag of 4 days. Predicted fluxes were also high when soil moisture was low (< 0.1 m^{-3} m^{-3}, frozen soil). For WTL, the predicted flux was generally high when WTL was high (> –45 cm), with the highest predicted flux on average for 4 days lagged WTL. The predicted flux for unlagged WTL was low at high WTL, while the predicted flux for unlagged WTL increased with decreasing WTL. N_2O flux was predicted to be the highest 4–7 days after precipitation with an average lag of 5 days between chambers when daily precipitation had been at least 5 mm.

For air and soil surface temperatures above 5 °C, the predicted fluxes increased with increasing temperature, with the highest predicted fluxes at air temperatures above 15 °C and soil temperatures above 10 °C. For air and soil temperatures (soil surface and 5 cm depth) below 0–2 °C, the predicted N_2O fluxes increased with decreasing temperature. In most chambers, the increase in predicted flux for soil 5 cm temperature at 0–2 °C was particularly strong. Responses between lagged and unlagged temperatures varied among chambers.

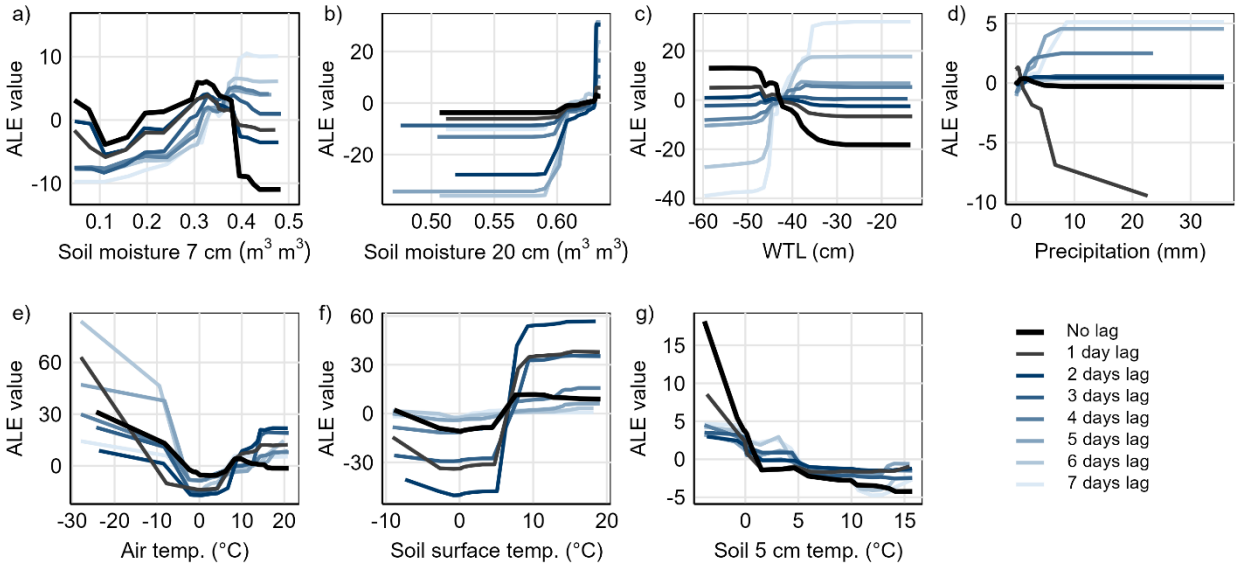

Figure 9: Response of predicted N_2O flux to different environmental conditions for Chamber 1 visualized using Accumulated Local Effects (ALE). Figures illustrate how the predicted N_2O flux values deviate from the mean predicted flux (ALE = 0) along the gradients of (a) soil moisture at 7 cm depth, (b) soil moisture at 20 cm depth, (c) water table level (WTL), (d) precipitation, (e) air temperature, (f) soil surface temperature and (g) soil temperature at 5 cm. ALE responses for unlagged and lagged variables (1–7 days) are included. ALE responses for Chambers 2–6 are presented in supplements (S7).

3.5. N_2O budgets

The annual N_2O budgets of individual chambers varied between 60 (Chamber 6) and 2110 mg N_2O m^{-2} y^{-1} (Chamber 1) when considering the three full measurement years 2016, 2017 and 2018 (Fig. 10, Tables S8). In 2016 and 2017, annual N_2O budgets were 1120–2110 mg N_2O m^{-2} y^{-1} in the high-flux chambers and 200–740 mg N_2O m^{-2} y^{-1} in the low-flux chambers. In 2018, the N_2O budgets were lower than 400 mg N_2O m^{-2} y^{-1} in all chambers. Winters and summers generally contributed the most to the annual N_2O budgets in all three years, with summers contributing on average 48 % and winters 34 % (Tables S8). The contributions of spring and autumn to the annual N_2O budgets were on average 10 % per season.

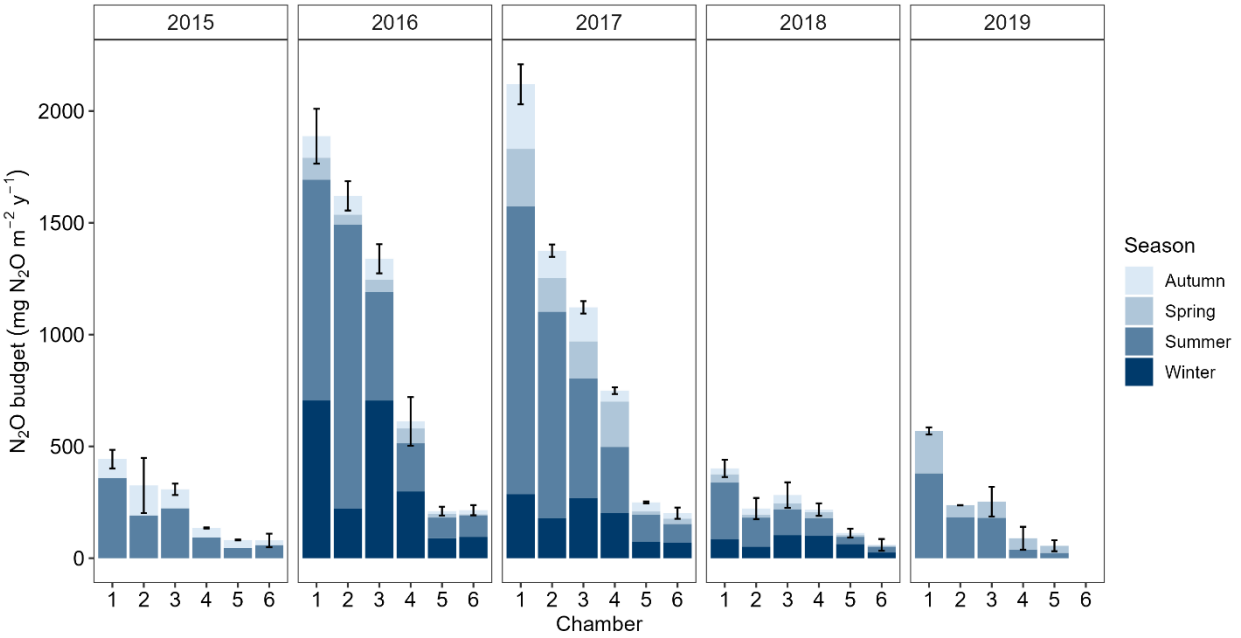

Figure 10: Annual N_2O budgets for each chamber and measurement year with seasonal contributions. The N_2O budget for 2015 only includes summer and autumn, and the N_2O budget for 2019 spring and summer. Measurements in Chamber 6 ended in early 2019 and no budget is shown for that year. Thermal seasons are used. Error bars denote total uncertainty related to the total N_2O budget of the year.

4. Discussion

The measured N_2O fluxes were relatively high compared to fluxes reported for other boreal and temperate forests on peat and mineral soils. The N_2O budgets of boreal peatland forests have mainly varied between 30 and 1200 mg N_2O m^{-2} y^{-1} (Arnold et al., 2005; Minkkinen et al, 2020; Butlers et al., 2023), and in a similar range also in temperate mineral soil forests (Papen and Butterbach-Bahl, 1999; Luo et al., 2012). The N_2O budgets of our six automatic chambers are unlikely able to represent the N_2O budget of the whole site, but the mean annual N_2O budget of the chamber area greater than 950 mg N_2O m^{-2} y^{-1} in the two full study years out of three underlines the role of drained nutrient-rich peatland forest as hotspots for N_2O emissions (Fig. 10).

Nutrient-rich peat with a relatively low C:N ratio likely explains the high N_2O budgets of the chamber area. Low C:N ratio may also have increased the sensitivity of the N_2O flux to temporal variation in soil conditions (Klemedtsson et al., 2005; Pihlatie et al., 2010). Although the selection harvest done at the site in the spring 2016 did not increase the N_2O budget of the harvested area compared to the control site according to Korkiakoski et al. (2020), the effect of the harvest on N_2O fluxes of individual chambers cannot be completely excluded. Since the N_2O budgets increased after harvesting in both the harvested and the control site (Korkiakoski et al., 2020), most of the increase in N_2O budgets in the years 2016 and 2017 is likely explained by year-to-year variation in environmental conditions.

4.1. Seasonal variation of N_2O fluxes

Winters were characterized by N_2O flux peaks occurring during both freezing and thawing (Fig. 6, 7 and S5), similar to those reported in earlier studies (Teepe et al., 2001; Maljanen et al., 2007; Maljanen et al., 2010). Freezing-related N_2O emissions are likely explained by N_2O production in the remaining unfrozen water films that have increased C and N content in the freezing soil (Maljanen et al., 2007; Congreves et al., 2018). Winter N_2O flux peaks were measured when soil frost reached at least the 5 cm depth, whereas during winters with only shallow frost (< 5 cm, winters 2017–2018 and 2018–2019), high N_2O fluxes were less common. This indicates the importance of frost depth for winter N_2O emissions. The importance of ground frost severity and depth has also been suggested by others in several ecosystems (Nielsen et al., 2001; Koponen and Martikainen, 2004; Maljanen et al., 2007; Luo et al., 2012). The importance of deeper soil freezing may indicate that the freezing-related N_2O fluxes mainly originate from the freezing peat rather than from the surface litter layer, unlike suggested by Pihlatie et al. (2007) in a nutrient-poor peatland forest. Low C:N ratio may have favored N_2O production in the nutrient-rich peat (Klemedtsson et al., 2005). Site-specific differences in nutrient availability may influence the sensitivity of winter N_2O fluxes to frost depth.

Winters with deeper soil frost and higher N_2O emissions (winters 2015–2016 and 2016–2017) were characterized by discontinuous and shallow snow cover and variable temperature conditions (Fig. 3 and 4). Shallow snow cover combined with alternating cold and warm weather in the first two winters of the study period have likely increased the number of freeze-thaw cycles and their intensity leading to higher total N_2O fluxes (Maljanen et al., 2007; Ruan and Robertson, 2017). The results suggest the possibility for increasing winter N_2O emissions from drained peat soils if winters continue to warm, the occurrence of extreme temperature fluctuations increases and snow cover in the southern boreal region becomes shallower.

Similar to freezing, soil thawing triggered N_2O emissions during winter freeze-thaw cycles, but emissions ceased within a few days of the onset of the thawing phase even if soil temperature continued to rise (Fig. 6 and S5). Similar short-term N_2O peaks in response to soil thawing have been measured also in laboratory experiments by Teepe et al. (2001), and Koponen and Martikainen (2004). Thaw-related emissions have often been explained by increased N availability in the thawing soil (Groffman et al., 2006; Wagner-Riddle et al., 2017), and the cause of the short pulse of N_2O flux during winter thawing might be related to the rapid use of labile N made available during the soil freezing period. Release of N_2O accumulated in the frozen soil might also explain some of the short-term N_2O flux peaks during thaw (Maljanen et al., 2007; Pihlatie et al., 2010). The response of N_2O fluxes to soil thaw during winter was weaker than the response especially to early winter soil freezing which highlights the importance of freezing-related N_2O emissions in the studied ecosystem.

Previously, several studies on both peat and mineral soils have emphasized the importance of thaw-related spring N_2O fluxes in the annual N_2O budgets, with pronounced spring N_2O flux peaks in some cases accounting for a large fraction of the annual budget (Pihlatie et al., 2010; Luo et al., 2012; Wang et al., 2023). In the present study, spring soil thaw triggered N_2O emissions, but emissions increased slowly with increasing soil temperature and peaked in late spring or summer, significantly later after soil thaw than reported in previous studies (Fig. 6 and S5). The strong temperature dependence of spring N_2O fluxes may indicate that the substrate for the spring N_2O production comes from the decomposing peat and litter in the warming soil. Temperature dependence of spring fluxes could be related

to drained peat soil, where the major source of N is known to be decomposing peat (Martikainen et al., 1993). Different responses to thawing in winter compared to spring might be related to decreasing availability of N from early winter towards spring (Koponen and Martikainen, 2004; Congreves et al., 2018), which also likely explains the tendency for stronger response to freeze-thaw cycles in early winter.

High-flux periods during the growing season, especially in the summer, were associated with precipitation events that increased soil moisture and raised WTL (Fig. 6, 7 and S5). These high-flux periods increased the total N_2O budget of the rainy summers (2016 and 2017), whereas the N_2O budget was low in the warm and dry summer 2018. Precipitation events may have increased the number of anoxic microsites in the soil, favoring N_2O production also through denitrification (Congreves et al., 2018). Fast peat decomposition in the warm soil during the summer likely reduced oxygen availability in the soil and increased N availability from the mineralizing peat resulting in high N_2O fluxes after summer rain events (Maljanen et al., 2003). Low N_2O fluxes during dry summer are likely explained by low microbial activity and substrate availability in the dry soil (Borken and Matzner, 2009; Congreves et al., 2018). Our results on summer and winter N_2O fluxes suggest that low N_2O fluxes during dry summers might offset the effect of the increasing winter N_2O fluxes on annual N_2O budgets if dry summers become more frequent in the warming climate.

N_2O fluxes during autumn were low and showed little year-to-year variability (Fig. 5, 6 and S5). Low autumn N_2O emissions have also been measured in previous studies (Maljanen et al., 2003; Luo et al., 2012), although Pihlatie et al. (2007) and Alm et al. (1999) found increased autumn N_2O fluxes after litter fall in drained peatland forests. The low contribution of autumn N_2O fluxes to annual emissions in the present study is probably explained by the more nutrient-rich peat and the lower importance of N_2O production in the litter layer in the total N_2O production (Martikainen et al., 1993; Pihlatie et al., 2007). The results indicate that the site-specific differences in the peat nutrient availability could alter the contributions of different seasons to annual N_2O budgets. High temporal variability of fluxes and greater sensitivity of N_2O fluxes to environmental conditions in nutrient-rich peatland forests are likely to increase the sensitivity of N_2O budgets to increasing variability in seasonal conditions in the changing climate.

4.2. Linkages to spatial variation

Lower fluxes from the three low-flux chambers (maximum flux < 400 μg N_2O m^{-2} h^{-1}) compared to high N_2O fluxes (maximum flux > 1100 μg N_2O m^{-2} h^{-1}) measured in the three high-flux chambers demonstrate the spatially variable nature of N_2O flux even on a small scale within a few meters (Groffman et al., 2009; Hénault et al., 2012; Jungkunst et al., 2012). What was notable was that the spatial differences in N_2O fluxes between chambers were persistent across years. The persistence of spatial variation implies that spatial variation of N_2O flux is controlled by long-term controls that persist throughout years with different weather conditions.

The long-term controls could include, for example, spatial variation in soil properties (e.g. pH, bulk density, availability of different forms of N) or placement of plant roots both of which have been suggested to influence the spatial variation in N_2O fluxes even at very small scales within the soil (Butterbach-Bahl et al., 2002; Jungkunst et al., 2012; Kuzyakov and Blagodatskaya, 2015). In the present study, the high-flux chambers had fewer trees nearby than low-flux chambers, and the distance to nearby trees was greater (Fig. 1, Table S1). Tree roots may have affected the

availability of different forms of nitrogen through nitrogen uptake and nitrogen inputs to soil (Kaiser et al., 2011; Kuzyakov and Blagodatskaya, 2015; Hu et al., 2016), resulting in higher fluxes further away from the trees in this case. Because trees affect the forest floor microclimate, ground vegetation and soil conditions through transpiration and by influencing the distribution of rainfall and light in the forest (Butterbach-Bahl et al., 2002; Aalto et al., 2022), variation in the tree cover may also have contributed to the spatio-temporal dynamics of N_2O fluxes. Although the distance to trees seemed to explain some of the spatial variation in N_2O flux, the spatial variation, especially within the small and high-flux chamber groups, remained unexplained. Ground vegetation was also not linked to spatial variation of N_2O. The results emphasize the importance of comprehensive soil sampling (e.g. N forms, bulk density, pH, C:N, root density) and chamber-specific measurements of environmental variables (e.g. soil moisture, soil temperature, WTL), when studying spatio-temporal variation of N_2O flux, especially in the forested study sites with variable microclimate.

Despite the large spatial variation in the N_2O flux, the high-flux periods identified for each chamber typically occurred at similar times, although the exact length and timing of the high-flux periods varied (Fig. 4, Table S4). Similarities in the temporal variation of fluxes suggest that temporal changes in the soil environmental conditions affected N_2O fluxes relatively similarly across space. In previous studies, temporal patterns within sites were either variable or common across space (Velthof et al., 2000; Krichels and Yang, 2019), with both findings mainly attributed to the spatio-temporal variation of soil moisture. Stronger similarities in the temporal variation of N_2O flux within the low and high-flux chamber groups indicate that some differences in the response of N_2O flux to environmental conditions may be related to the overall spatial variation of the flux.

4.3 Delayed responses

The results indicate that N_2O flux has a delayed response to precipitation events with peak N_2O fluxes measured on average 4 days after soil moisture and WTL peaks, and 5 days after rainfall (Fig. 9 and S7). Studies mostly conducted on mineral soils in laboratories have found short time lags from the onset of anaerobiosis or water saturation to the highest measured N_2O production, with lags ranging from few hours to less than two days (Firestone and Tiedje, 1979; Smith and Tiedje, 1979; Russow et al., 2000; Song et al., 2019). Compared to the previous studies, the observed lag times are long, with indication for even longer lags than seven days in some chambers.

The present data only allow us to hypothesize the causes of the long lag times after precipitation events. The ability of peat to retain moisture and thus anaerobic microsites in the soil means that anaerobic conditions for denitrification are maintained and the possible co-occurrence of nitrification and denitrification can last for longer than in most mineral soils (Päivänen, 1973; Wrage et al., 2001; Walczak et al., 2002). The highest N_2O fluxes during the growing season were reached on intermediate soil moisture (0.3–0.4 m^{-3} m^{-3}) after the soil had started to drain and WTL had started to decrease after a precipitation event (Fig. 7 and 9, S7). Based on this study and previous laboratory studies, we suggest that after a period of high N_2O reduction activity and therefore relatively low N_2O fluxes from denitrification in the wet soil soon after rain, N_2O production in the draining soil increased (Firestone and Tiedje, 1979; Russow et al., 2000; Congreves et al., 2018). As soil continued to drain, conditions for simultaneous nitrification and denitrification became optimal (Bateman and Baggs, 2005; Wang et al., 2021; Song et al., 2022), further increasing

573 N_2O production and leading to the peak N_2O flux some days after rain. The ability of peat to retain moisture could
574 extend the time for soil drainage after rainfall and thus time before optimal conditions for N_2O production are reached.
575 Hydrophobic properties of dry peat soils can also extend the time before N_2O fluxes respond to soil wetting (Borken
576 and Matzner, 2009) contributing to longer lag times. To determine exact lag times in response to soil moisture peaks,
577 chamber-specific soil moisture data would be required.

578 Although models were not run for different seasons separately, the response of N_2O fluxes to precipitation
579 events seemed to be slower during autumn and resulted in lower N_2O flux peaks (Fig. 6 and S5). Lower temperatures
580 in autumn likely decreased microbial activity and mineralization of N from decomposing peat, which could explain
581 lower fluxes and slower response of N_2O fluxes to precipitation events in autumn (Holtan-Hartwig et al., 2002).
582 Chamber differences in the lag times associated with precipitation events and differences in the variable importance
583 of different environmental variables (Fig. 8 and S6) may also indicate varying sensitivities of N_2O production to
584 spatially varying soil conditions. These differences may be related to different microbial community, substrate
585 availability or soil properties that have been identified as important controls of N_2O production (Hénault et al., 2012;
586 Butterbach-Bahl et al., 2013; Hu et al., 2015) and are likely to shape the response of N_2O production to environmental
587 conditions.
588

589 ## 5. Conclusions

590 This study shows high temporal and spatial variability in peatland forest N_2O fluxes with persistent spatial
591 patterns across years with different environmental conditions. The temporal variation of N_2O flux was strongly
592 influenced by seasonal weather conditions, especially precipitation, snow depth and drought. Temporally varying soil
593 conditions affect N_2O fluxes through complex responses that include delayed responses to soil wetting. Interactions
594 between spatially and temporally varying soil conditions, such as temperature, further shape the spatio-temporal
595 patterns of N_2O flux. The considerable small-scale spatial variation in N_2O fluxes is likely to be influenced by
596 relatively long-term controls such as soil properties and positioning of trees.

597 The observed high N_2O fluxes from the peatland forest highlight the role of nutrient-rich drained peat soils
598 as hotspots for N_2O emissions in the boreal region. The dependence of N_2O budgets on seasonally varying weather
599 conditions suggests high sensitivity of peatland forest N_2O budgets to changing climate. Winter N_2O emissions will
600 likely increase in the future due to warming winters with shallow and discontinuous snow cover. Summer N_2O
601 emissions may decrease and possibly offset the effect of warming winters on annual N_2O budgets in dry years. Year-
602 to-year variation in N_2O emissions will likely increase as extreme weather events are predicted to become more
603 frequent.
604

605 ## 6. Appendices

606 ### Appendix A. Thermal seasons

607 Thermal winter was the season with daily mean air temperatures persistently below 0 °C and thermal summer
608 season with daily mean air temperatures persistently above 10 °C (Ruosteenoja et al., 2016; Finnish Meteorological

Institute, 2023). During spring and autumn, temperatures varied between 0–10 °C. Cumulative temperature sums of daily mean temperatures were then used to identify the starting days of the thermal seasons at which temperature went persistently above or below the seasonal temperature threshold (0 or 10 °C). The starting day of the thermal winter was the day after the annual cumulative temperature sum reached the maximum. The starting day of the thermal spring was the day after the minimum cumulative temperature sum was reached. Starting days of thermal summer and autumn were calculated similarly but by extracting 10 °C from the air temperatures before calculating the cumulative temperature sum (modified temperature sum). The day after the minimum modified temperature sum was reached was defined as the starting date of the summer, while the maximum modified cumulative temperature pointed the onset of thermal autumn.

Appendix B. Evaluating the model performance

R_2 of the chamber-specific models used in the analyses varied between 0.72 and 0.85 in OOB data, and between 0.60 and 0.69 in training period evaluation data (30 % of training period data) (Table B1). When predicting N_2O fluxes outside the training period (fourth measurement year), R_2 varied between 0.02 and 0.69. The performance of gap-filling models was tested only using OOB data and evaluation data within the whole study period (30 % of data). For gap-filling models, R_2 in OOB data varied between 0.71 and 0.84, while R_2 in evaluation data varied between 0.67 and 0.78 (Table B2).

For the models used in the analysis, the poor prediction accuracy outside of the training period, especially in Chambers 3, 4, and 6, was likely due to overestimation of the general flux level during the relatively dry year 2019, which was excluded from the training period (Fig. S9). The model was also unable to predict anomalous high-flux period in low-flux winter 2018–2019 in Chamber 5 likely due to a lack of chamber-specific soil temperature data deeper in the soil. The temporal patterns of the flux otherwise followed temporal patterns of measured fluxes relatively well. Poor prediction accuracy outside the training period in part of the chambers indicates that predicting N_2O fluxes to a year with distinct environmental conditions compared to the years in the training data may lead to large under or overestimation of N_2O fluxes. The used models could benefit from additional explanatory variables, such as redox potential or the availability of different forms of nitrogen (Rubol et al., 2012; Saha et al., 2020). Including additional soil variables in the model could decrease the need to have excessively large model training periods to accurately predict and gap-fill N_2O fluxes.

Table B1: Model performance in evaluation datasets. Out-of-bag (OOB) data refers to data left outside model training in random forest with conditional inference trees, evaluation data within the training period refers to 30 % of data randomly left aside for model evaluation and evaluation data outside the training period refers to the fourth measurement year outside model training period.

Chamber	Evaluation data	RMSE	R^2
1	OOB	138.8	0.75
	Within training period	134.9	0.60
	Outside training period	113.7	0.67

2	OOB	105.7	0.84
	Within training period	106.0	0.69
	Outside training period	85.1	0.69
3	OOB	81.0	0.72
	Within training period	93.7	0.64
	Outside training period	75.7	0.02
4	OOB	36.3	0.83
	Within training period	29.5	0.77
	Outside training period	56.6	0.01
5	OOB	14.5	0.85
	Within training period	12.7	0.65
	Outside training period	22.0	0.33
6	OOB	10.2	0.85
	Within training period	10.3	0.68
	Outside training period	17.0	0.03

Table B2: Performance of gap-filling models on evaluation datasets. Out-of-bag (OOB) data refers to data left outside model training in random forest with conditional inference trees and evaluation data within the training period refers to 30 % of training period data that was randomly left aside for model evaluation. The training period of gap-filling models covers the total study period (4.5 years).

Chamber	Evaluation data	RMSE	R^2
1	OOB	118.3	0.80
	Within training period	124.7	0.67
2	OOB	90.2	0.84
	Within training period	86.6	0.78
3	OOB	80.7	0.74
	Within training period	62.1	0.69
4	OOB	30.3	0.83
	Within training period	28.6	0.76
5	OOB	16.7	0.71
	Within training period	14.0	0.71
6	OOB	9.9	0.82
	Within training period	9.7	0.72

7. Data availability

Flux data and supporting environmental data are available at: https://doi.org/10.5281/zenodo.8142188 (Rautakoski et al., 2023a). Simplified R code of the machine learning part of the study is made freely available at:

https://github.com/helenemilii/N2O_modeling. Python codes used in flux calculation and R codes used in data analysis are available from the corresponding author by request.

8. Supplement

The supplement of the article is available at: https://doi.org/10.5281/zenodo.10533480 (Rautakoski et al., 2023b).

9. Author Contributions

AL, MA, MK and PO set up the study design. Field maintenance of measurement systems was carried out by MK, AL and PO. Fluxes were calculated by MK and filtered by HR. Data analysis, modeling and writing of the article were done by HR with the support of AL and other co-authors.

10. Competing interests

The authors declare that they have no conflict of interest.

11. Acknowledgments

We thank the Academy of Finland (Biogeochemical and biophysical feedbacks from forest harvesting to climate change – BiBiFe, Grant no. 324259; Managing Forests for Climate Change Mitigation – FORCLIMATE, Grant no. 347794), the Maj and Tor Nessling foundation (Grant no. 201700450) and Wet Horizons (Horizon Europe GAP-101056848) for funding the work. We also thank for the support by the ACCC Flagship funded by the Academy of Finland (Grant no. 337552) and the Ministry of Transport and Communications through the Integrated Carbon Observation System (ICOS) and ICOS Finland. DeepL Write (DeepL SE, 2023) was used to improve the language of the article.

12. References

Aalto, J., Tyystjärvi, V., Niittynen, P., Kemppinen, J., Rissanen, T., Gregow, H., and Luoto, M.: Microclimate temperature variations from boreal forests to the tundra, Agric. For. Meteorol., 323, 109037, https://doi.org/10.1016/j.agrformet.2022.109037, 2022

Abd Elrahman, S. M., and Abraham, A.: A review of class imbalance problem. J. Netw. Innov. Comput., 1, 332–340, 2013

Apley, D. W., and Zhu, J.: Visualizing the effects of predictor variables in black box supervised learning models. Journal of the Royal Statistical Society Series B: Stat. Methodol., 82(4), 1059-1086, https://doi.org/10.1111/rssb.12377, 2020

Alm, J., Saarnio, S., Nykänen, H., Silvola, J., and Martikainen, P.: Winter CO_2, CH_4 and N_2O fluxes on some natural and drained boreal peatlands, Biogeochemistry, 44, 163–186, https://doi.org/10.1007/BF00992977, 1999

Anthony, T. L., and Silver, W. L.: Hot moments drive extreme nitrous oxide and methane emissions from agricultural peatlands, Glob. Change Biol., 27(20), 5141–5153, https://doi.org/10.1111/gcb.15802, 2021

Arnold, K. V., Weslien, P., Nilsson, M., Svensson, B. H., and Klemedtsson, L.: Fluxes of CO_2, CH_4 and N_2O from drained coniferous forests on organic soils, For. Ecol. Manag., 210(1-3), 239–254, https://doi.org/10.1016/j.foreco.2005.02.031, 2005

Barton, L., Wolf, B., Rowlings, D., Scheer, C., Kiese, R., Grace, P., Stefanova, K., and Butterbach-Bahl, K.: Sampling frequency affects estimates of annual nitrous oxide fluxes, Sci. Rep., 5(1), 15912, https://doi.org/10.1038/srep15912, 2015

Bateman, E. J., and Baggs, E. M.: Contributions of nitrification and denitrification to N_2O emissions from soils at different water-filled pore space, Biol. Fertil. Soils, 41(6), 379–388, https://doi.org/10.1007/s00374-005-0858-3, 2005

Bollmann, A., and Conrad, R.: Influence of O2 availability on NO and N_2O release by nitrification and denitrification in soils, Glob. Change Biol., 4(4), 387–396, https://doi.org/10.1046/j.1365-2486.1998.00161.x, 1998

Borken, W., and Matzner, E.: Reappraisal of drying and wetting effects on C and N mineralization and fluxes in soils, Glob. Change Biol., 15(4), 808–824, https://doi.org/10.1111/j.1365-2486.2008.01681.x, 2009

Breiman, L.: Random forests, Mach. Learn., 45, 5–32, https://doi.org/10.1023/A:1010933404324, 2001

Butlers, A., Lazdiņš, A., Kalēja, S., Purviņa, D., Spalva, G., Saule, G., and Bārdule, A.: CH_4 and N_2O emissions of undrained and drained nutrient-rich organic forest soil, Forests, 14(7), 1390, https://doi.org/10.3390/f14071390, 2023

Butterbach-Bahl, K., Rothe, A., and Papen, and H.: Effect of tree distance on N_2O and CH_4 fluxes from soils in temperate forest ecosystems, Plant Soil, 240, 91–103, https://doi.org/10.1023/A:1015828701885, 2002

Butterbach-Bahl, K., Baggs, E. M., Dannenmann, M., Kiese, R., and Zechmeister-Boltenstern, S.: Nitrous oxide emissions from soils: how well do we understand the processes and their controls?, Philos. Trans. R. Soc. Lond., B, Biol. Sci., 368(1621), 20130122, https://doi.org/10.1098/rstb.2013.0122, 2013

Congreves, K. A., Wagner-Riddle, C., Si, B. C., and Clough, T. J.: Nitrous oxide emissions and biogeochemical responses to soil freezing-thawing and drying-wetting, Soil Biol. Biochem., 117, 5–1, https://doi.org/10.1016/j.soilbio.2017.10.040, 2018

Davidson, E. A., and Kanter, D.: Inventories and scenarios of nitrous oxide emissions, Environ. Res. Lett., 9(10), 105012, https://doi.org/10.1088/1748-9326/9/10/105012, 2014

Finnish Meteorological Institute: https://en.ilmatieteenlaitos.fi/seasons-in-finland, last access 11 July 2023

Firestone, M., and Tiedje, J.: Temporal change in nitrous oxide and dinitrogen from denitrification following onset of anaerobiosis, Appl. Environ. Microbiol., 38(4), 673–679, https://doi.org/10.1128/aem.38.4.673-679.1979, 1979

Forster, P., Storelvmo, T., Armour, K., Collins, W., Dufresne, J.-L., Frame, D., Lunt, D. J., Mauritsen, T., Palmer, M. D., Watanabe, M., Wild, M., and Zhang, H.: The Earth's Energy Budget, Climate Feedbacks, and Climate sensitivity. In Climate Change 2021: The Physical Science Basis. Contribution of Working Group I to the Sixth Assessment Report of the Intergovernmental Panel on Climate Change, edited by: Masson-Delmotte, V., Zhai, P., Pirani, A., Connors, S. L., Péan, C., Berger, S., Caud, N., Chen, Y., Goldfarb, L.,

Gomis, M. I., Huang, M., Leitzell, K., Lonnoy, E., Matthews, J. B. R., Maycock, T.K., Waterfield, T., Yelekçi, O., Yu, R., and Zhou, B., Cambridge University Press, Cambridge, United Kingdom and New York, NY, USA, pp. 923–1054, doi:10.1017/9781009157896.009, 2021

Gerin, S., Vekuri, H., Liimatainen, M., Tuovinen, J. P., Kekkonen, J., Kulmala, L., Laurila, T., Linkosalmi, M., Liski, J., Joki-Tokola, E., and Lohila, A.: Two contrasting years of continuous N_2O and CO_2 fluxes on a shallow-peated drained agricultural boreal peatland. Agric. For. Meteorol., 341, 109630, https://doi.org/10.1016/j.agrformet.2023.109630, 2023

Giltrap, D. L., Berben, P., Palmada, T., and Saggar, S.: Understanding and analysing spatial variability of nitrous oxide emissions from a grazed pasture, Agric. Ecosyst. Environ., 186, 1–10, https://doi.org/10.1016/j.agee.2014.01.012, 2014

Grace, P. R., Weerden, T. J., Rowlings, D. W., Scheer, C., Brunk, C., Kiese, R., Butterbach-Bahl, K., Rees, R. M., Robertson, G. P., and Skiba, U. M.: Global Research Alliance N_2O chamber methodology guidelines: Considerations for automated flux measurement, J. Environ. Qual., 49(5), 1126–1140, https://doi.org/10.1002/jeq2.20124, 2020

Groffman, P. M., Hardy, J. P., Driscoll, C. T., and Fahey, T. J.: Snow depth, soil freezing, and fluxes of carbon dioxide, nitrous oxide and methane in a northern hardwood forest. Glob. Change Biol., 12(9), 1748-1760., https://doi.org/10.1111/j.1365-2486.2006.01194.x, 2006

Groffman, P. M., Butterbach-Bahl, K., Fulweiler, R. W., Gold, A. J., Morse, J. L., Stander, E. K., Tague, C., Tonitto, C., and Vidon, P.: Challenges to incorporating spatially and temporally explicit phenomena (hotspots and hot moments) in denitrification models, Biogeochemistry, 93(1-2), 49–77, https://doi.org/10.1007/s10533-008-9277-5, 2009

Hénault, C., Grossel, A., Mary, B., Roussel, M., and Léonard, J.: Nitrous oxide emission by agricultural soils: a review of spatial and temporal variability for mitigation, Pedosphere, 22(4), 426–433, https://doi.org/10.1016/S1002-0160(12)60029-0, 2012

Holtan-Hartwig, L., Dörsch, P., and Bakken, L. R.: Low temperature control of soil denitrifying communities: kinetics of N_2O production and reduction, Soil Biol. Biochem., 34(11), 1797–1806, https://doi.org/10.1016/S0038-0717(02)00169-4, 2002

Hothorn, T., Hornik, K., and Zeileis, A.: Unbiased recursive partitioning: A Conditional inference framework, J. Comput. Graph. Stat., 15(3), 651–674, https://doi.org/10.1198/106186006X133933, 2006

Hu, H. W., Chen, D., and He, J. Z.: Microbial regulation of terrestrial nitrous oxide formation: understanding the biological pathways for prediction of emission rates, FEMS Microbiol. Rev., 39(5), 729–749, https://doi.org/10.1093/femsre/fuv021, 2015

Hu, X., Liu, L., Zhu, B., Du, E., Hu, X., Li, P., Zhou, Z., Ji, C., Zhu, J., Shen, H., and Fang, J.: Asynchronous responses of soil carbon dioxide, nitrous oxide emissions and net nitrogen mineralization to enhanced fine root input, Soil Biol. and Biochem., 92, 67–78, http://dx.doi.org/10.1016/j.soilbio.2015.09.019, 2016

759 Huttunen, J. T., Nykänen, H., Martikainen, P. J., and Nieminen, M.: Fluxes of nitrous oxide and methane from
760 drained peatlands following forest clear-felling in southern Finland, Plant Soil, 255(2), 457–462,
761 https://doi.org/10.1023/A:1026035427891, 2003
762 Ju, X., and Zhang, C.: Nitrogen cycling and environmental impacts in upland agricultural soils in North China: A
763 review, J. Integr. Agric., 16(12), 2848–2862, https://doi.org/10.1016/S2095-3119(17)61743-X, 2017
764 Jungkunst, H. F., Bargsten, A., Timme, M., and Glatzel, S.: Spatial variability of nitrous oxide emissions in an
765 unmanaged old-growth beech forest, J. Plant. Nutr. Soil Sci., 175(5), 739–749,
766 https://doi.org/10.1002/jpln.201100412, 2012
767 Kaiser, C., Fuchslueger, L., Koranda, M., Gorfer, M., Stange, C. F., Kitzler, B., Rasche, F., Strauss, J., Sessitsch, A.,
768 Zechmeister-Boltenstern, S., and Richter, A.: Plants control the seasonal dynamics of microbial N cycling
769 in a beech forest soil by belowground C allocation, Ecology, 92(5), 1036-1051, https://doi.org/10.1890/10-
770 1011.1, 2011
771 Klemedtsson, L., Von Arnold, K., Weslien, P., and Gundersen, P.: Soil CN ratio as a scalar parameter to predict
772 nitrous oxide emissions, Glob. Change Biol., 11(7), 1142–1147, https://doi.org/10.1111/j.1365-
773 2486.2005.00973.x, 2005
774 Koponen, H. T., and Martikainen, P. J.: Soil water content and freezing temperature affect freeze–thaw related N_2O
775 production in organic soil, Nutr. Cycl. Agroecosystems, 69, 213–219,
776 https://doi.org/10.1023/B:FRES.0000035172.37839.24, 2004
777 Korhonen, K. T., Ahola, A., Heikkinen, J., Henttonen, H. M., Hotanen, J. P., Ihalainen, A., Melin, M., Pitkänen, J.,
778 Räty, M., Sirviö, M., and Strandström, M.: Forests of Finland 2014–2018 and their development 1921–
779 2018, Silva Fenn., 55(5), 10662, https://doi.org/10.14214/sf.10662, 2021
780 Korkiakoski, M., Tuovinen, J. P., Aurela, M., Koskinen, M., Minkkinen, K., Ojanen, P., Penttilä, T., Rainne, J.,
781 Laurila, T., and Lohila, A.: Methane exchange at the peatland forest floor – automatic chamber system
782 exposes the dynamics of small fluxes, Biogeosciences, 14(7), 1947–1967, https://doi.org/10.5194/bg-14-
783 1947-2017, 2017
784 Korkiakoski, M., Tuovinen, J. P., Penttilä, T., Sarkkola, S., Ojanen, P., Minkkinen, K., Rainne, J., Laurila, T., and
785 Lohila, A.: Greenhouse gas and energy fluxes in a boreal peatland forest after clear-cutting,
786 Biogeosciences, 16(19), 3703–3723, https://doi.org/10.5194/bg-16-3703-2019, 2019
787 Korkiakoski, M., Ojanen, P., Penttilä, T., Minkkinen, K., Sarkkola, S., Rainne, J., Laurila, T., and Lohila, A.: Impact
788 of partial harvest on CH_4 and N_2O balances of a drained boreal peatland forest, Agric. For. Meteorol., 295,
789 108168, https://doi.org/10.1016/j.agrformet.2020.108168, 2020
790 Korkiakoski, M., Ojanen, P., Tuovinen, J. P., Minkkinen, K., Nevalainen, O., Penttilä, T., Aurela, M., Laurila, T.,
791 and Lohila, A.: Partial cutting of a boreal nutrient-rich peatland forest causes radically less short-term on-
792 site CO_2 emissions than clear-cutting, Agric. For. Meteorol., 332, 109361,
793 https://doi.org/10.1016/j.agrformet.2023.109361, 2023
794 Koskinen, M., Minkkinen, K., Ojanen, P., Kämäräinen, M., Laurila, T., and Lohila, A.: Measurements of CO_2
795 exchange with an automated chamber system throughout the year: challenges in measuring night-time

respiration on porous peat soil, Biogeosciences, 11(2), 347–363, https://doi.org/10.5194/bg-11-347-2014, 2014

Krichels, A. H., and Yang, W. H.: Dynamic controls on field-scale soil nitrous oxide hot spots and hot moments across a microtopographic gradient, J. Geophys. Res. Biogeosci., 124(11), 3618–3634, https://doi.org/10.1029/2019JG005224, 2019

Kuzyakov, Y., and Blagodatskaya, E.: Microbial hotspots and hot moments in soil: Concept & review, Soil Biol. Biochem., 83, 184–199, https://doi.org/10.1016/j.soilbio.2015.01.025, 2015

Laine, J., Silvola, J., Tolonen, K., Alm, J., Nykänen, H., Vasander, H., Sallantaus, T., Savolainen, I., Sinisalo, J., and Martikainen, P. J.: Effect of water-level drawdown on global climatic warming: Northern peatlands, Ambio, 25(3), 179–184, http://www.jstor.org/stable/4314450, 1996

Leppelt, T., Dechow, R., Gebbert, S., Freibauer, A., Lohila, A., Augustin, J., Drösler, M., Fiedler, S., Glatzel, S., Höper, H., Järveoja, J., Lærke, P. E., Maljanen, M., Mander, Ü., Mäkiranta, P., Minkkinen, K., Ojanen, P., Regina, K., and Strömgren, M.: Nitrous oxide emission budgets and land-use-driven hotspots for organic soils in Europe, Biogeosciences, 11(23), 6595–6612, https://doi.org/10.5194/bg-11-6595-2014, 2014

Liaw, A., and Wiener, M.: Classification and Regression by randomForest. R News 2(3), 18–22, https://CRAN.R-project.org/doc/Rnews/, 2002

Lin, F., Zuo, H., Ma, X., and Ma, L.: Comprehensive assessment of nitrous oxide emissions and mitigation potentials across European peatlands, Environ. Pollut., 301, 119041, https://doi.org/10.1016/j.envpol.2022.119041, 2022

Luo, G. J., Brüggemann, N., Wolf, B., Gasche, R., Grote, R., and Butterbach-Bahl, K.: Decadal variability of soil CO_2, NO, N_2O and CH_4 fluxes at the Höglwald Forest, Germany, Biogeosciences, 9(5), 1741–1763, https://doi.org/10.5194/bg-9-1741-2012, 2012

Maljanen, M., Liikanen, A., Silvola, J., and Martikainen, P. J.: Nitrous oxide emissions from boreal organic soil under different land-use, Soil Biol. Biochem., 35(5), 689–700, https://doi.org/10.1016/S0038-0717(03)00085-3, 2003

Maljanen, M., Kohonen, A. R., Virkajärvi, P., and Martikainen, P. J.: Fluxes and production of N_2O, CO2 and CH4 in boreal agricultural soil during winter as affected by snow cover. Tellus B: Chemical and Physical Meteorology, 59(5), 853-859, https://doi.org/ 10.1111/j.1600-0889.2007.00304.x, 2007

Maljanen, M., Hytönen, J., and Martikainen, P. J.: Cold-season nitrous oxide dynamics in a drained boreal peatland differ depending on land-use practice, Can. J. For. Res., 40(3), 565–572, https://doi.org/10.1139/X10-004, 2010

Martikainen, P. J., Nykänen, H., Crill, P., and Silvola, J.: Effect of a lowered water table on nitrous oxide fluxes from northern peatlands, Nature, 366(6450), 51–53, https://doi.org/10.1038/366051a0, 1993

Minkkinen, K., Ojanen, P., Koskinen, M., and Penttilä, T.: Nitrous oxide emissions of undrained, forestry-drained, and rewetted boreal peatlands, For. Ecol. Manag., 478, 118494, https://doi.org/10.1016/j.foreco.2020.118494, 2020

Molodovskaya, M., Singurindy, O., Richards, B. K., Warland, J., Johnson, M. S., and Steenhuis, T. S.: Temporal variability of nitrous oxide from fertilized croplands: Hot moment analysis, Soil Sci. Soc. Am. J., 76(5), 1728–1740, https://doi.org/10.2136/sssaj2012.0039, 2012

Nielsen, C. B., Groffman, P. M., Hamburg, S. P., Driscoll, C. T., Fahey, T. J., and Hardy, J. P.: Freezing effects on carbon and nitrogen cycling in northern hardwood forest soils, Soil Sci. Soc. Am. J., 65(6), 1723–1730, https://doi.org/10.2136/sssaj2001.1723, 2001

Nickerson, N.: Evaluating gas emission measurements using Minimum Detectable Flux (MDF). Eosense Inc., Dartmouth, Nova Scotia, Canada, https://eosense.com/wp-content/uploads/2019/11/Eosense-white-paper-Minimum-Detectable-Flux.pdf, 2016

Ojanen, P., Minkkinen, K., Alm, J., and Penttilä, T.: Soil–atmosphere CO_2, CH_4 and N_2O fluxes in boreal forestry-drained peatlands, For. Ecol. Manag., 260(3), 411–421, https://doi.org/10.1016/j.foreco.2010.04.036, 2010

Olden, J. D., Lawler, J. J., and Poff, N. L.: Machine learning methods without tears: A primer for ecologists, Q. Rev. Biol., 83(2), 171–193, https://doi.org/10.1086/587826, 2008

Pavelka, M., Acosta, M., Kiese, R., Altimir, N., Brümmer, C., Crill, P., Darenova1, E., Fub, R., Gielen, B., Graf, A., Klemedtsson, L., Lohila, A., Longdoz, B., Lindroth, A., Nilsson, M., Maraňón Jiménez, S., Merbold, L., Montagnani, L., Peichl, M., Pihlatie, M. Pumpanen, J., Serrano Ortiz, P.,Silvennoinen, H., Skiba, U., Vestin, P., Weslien, P., Janous, D., and Kutsch, W.: Standardisation of chamber technique for CO_2, N_2O and CH_4 fluxes measurements from terrestrial ecosystems. Int. Agrophys. 32, 569-587, https://doi.org/10.1515/intag-2017-0045, 2018

Päivänen, J.: Hydraulic conductivity and water retention in peat soils, Acta Forestalia Fennica, 129(1–70), 1973

Papen, H., and Butterbach-Bahl, K.: A 3-year continuous record of nitrogen trace gas fluxes from untreated and limed soil of a N-saturated spruce and beech forest ecosystem in Germany 1. N_2O emissions, J. Geophys. Res. Atmos., 104(D15), 18487–18503, https://doi.org/10.1029/1999JD900293, 1999

Pärn, J., Verhoeven, J. T. A., Butterbach-Bahl, K., Dise, N. B., Ullah, S., Aasa, A., Egorov, S., Espenberg, M., Järveoja, J., Jauhiainen, J., Kasak, K., Klemedtsson, L., Kull, A., Laggoun-Défarge, F., Lapshina, E. D., Lohila, A., Lõhmus, K., Maddison, M., Mitsch, W. J., … Mander, Ü.: Nitrogen-rich organic soils under warm well-drained conditions are global nitrous oxide emission hotspots, Nat. Commun., 9(1), 1135, https://doi.org/10.1038/s41467-018-03540-1, 2018

Pihlatie, M., Pumpanen, J., Rinne, J., Ilvesniemi, H., Simojoki, A., Hari, P., and Vesala, T.: Gas concentration driven fluxes of nitrous oxide and carbon dioxide in boreal forest soil, Tellus B Chem. Phys. Meteorol., 59(3), 458–469, https://doi.org/10.1111/j.1600-0889.2007.00278.x, 2007

Pihlatie, M., Kiese, R., Brüggemann, N., Butterbach-Bahl, K., Kieloaho, A.-J., Laurila, T., Lohila, A., Mammarella, I., Minkkinen, K., Penttilä, T., Schönborn, J., and Vesala, T.: Greenhouse gas fluxes in a drained peatland forest during spring frost-thaw event, Biogeosciences, 7(5), 1715–1727, https://doi.org/10.5194/bg-7-1715-2010, 2010

Rautakoski, H., Korkiakoski, M., Aurela, M., Minkkinen, K., Ojanen, P., and Lohila, A.: 4.5 years of peatland forest N_2O flux data data measured using automatic chambers, Zenodo, https://doi.org/ 10.5281/zenodo.8142188, 2023a

Rautakoski, H., Korkiakoski, M., Aurela, M., Minkkinen, K., Ojanen, P., and Lohila, A.: Supplementary material to the article "Exploring temporal and spatial variation of nitrous oxide flux using several years of peatland forest automatic chamber data", Zenodo, https://doi.org/10.5281/zenodo.10533480, 2023b

R Core Team: R: A language and environment for statistical computing, R Foundation for Statistical Computing, Vienna, Austria, https://www.R-project.org/, 2021

Reay, D. S., Davidson, E. A., Smith, K. A., Smith, P., Melillo, J. M., Dentener, F., and Crutzen, P. J.: Global agriculture and nitrous oxide emissions, Nat. Clim. Chang., 2(6), 410–416, https://doi.org/10.1038/nclimate1458, 2012

Regina, K., Martikainen, P. J., and Silvola, J.: Mechanisms of N_2O and NO production in the soil profile of a drained and forested peatland, as studied with acetylene, nitrapyrin and dimethyl ether, Biol. Fertil. Soils, 27(2), 205–210, https://doi.org/10.1007/s003740050421, 1998

Risk, N., Snider, D., and Wagner-Riddle, C.: Mechanisms leading to enhanced soil nitrous oxide fluxes induced by freeze–thaw cycles, Can. J. Soil Sci., 93(4), 401–414, https://doi.org/10.4141/cjss2012-071, 2013

Ruan, L., and Robertson, G. P.: Reduced snow cover increases wintertime nitrous oxide (N_2O) emissions from an agricultural soil in the upper U.S. Midwest, Ecosystems, 20(5), 917–927, https://doi.org/10.1007/s10021-016-0077-9, 2017

Rubol, S., Silver, W. L., and Bellin, A.: Hydrologic control on redox and nitrogen dynamics in a peatland soil, Sci. Total Environ., 432, 37–46, https://doi.org/10.1016/j.scitotenv.2012.05.073, 2012

Ruosteenoja, K., Räisänen, J., Venäläinen, A., and Kämäräinen, M.: Projections for the duration and degree days of the thermal growing season in Europe derived from CMIP5 model output. Int. J. Climatol., 36(8), 3039–3055. https://doi.org/10.1002/joc.4535, 2016

Russow, R., Sich, I., and Neue, H. U.: The formation of the trace gases NO and N_2O in soils by the coupled processes of nitrification and denitrification: results of kinetic 15N tracer investigations. Chem. Glob. Change Sci., 2(3–4), 359–366, https://doi.org/10.1016/S1465-9972(00)00012-X, 2000

Saha, D., Basso, B., and Robertson, G. P.: Machine learning improves predictions of agricultural nitrous oxide (N_2O) emissions from intensively managed cropping systems, Environ. Res. Lett., 16(2), 024004, https://doi.org/10.1088/1748-9326/abd2f3, 2021

Shakoor, A., Shahzad, S. M., Chatterjee, N., Arif, M. S., Farooq, T. H., Altaf, M. M., Tufail, M. A., Dar, A. A., and Mehmood, T.: Nitrous oxide emission from agricultural soils: Application of animal manure or biochar? A global meta-analysis, J. Environ. Manage., 285, 112170, https://doi.org/10.1016/j.jenvman.2021.112170, 2021

Sharma, S., Szele, Z., Schilling, R., Munch, J. C., and Schloter, M.: Influence of freeze-thaw stress on the structure and function of microbial communities and denitrifying populations in soil. Appl. Environ. Microbiol., 72(3), 2148-2154, https://doi.org/ 10.1128/AEM.72.3.2148-2154.2006, 2006

Smith, M., and Tiedje, J.: Phases of denitrification following oxygen depletion in soil, Soil Biol. Biochem., 11, 261–267, https://doi.org/10.1016/0038-0717(79)90071-3, 1979

Song, X., Ju, X., Topp, C. F. E., and Rees, R. M.: Oxygen regulates nitrous oxide production directly in agricultural soils, Environ. Sci. Technol., 53(21), 12539–12547, https://doi.org/10.1021/acs.est.9b03089, 2019

Song, X., Wei, H., Rees, R. M., and Ju, X.: Soil oxygen depletion and corresponding nitrous oxide production at hot moments in an agricultural soil, Environ. Pollut., 292, 118345, https://doi.org/10.1016/j.envpol.2021.118345, 2022

Strobl, C., Boulesteix, A.-L., Zeileis, A., and Hothorn, T.: Bias in random forest variable importance measures: Illustrations, sources and a solution, BMC Bioinform., 8(1), 25, https://doi.org/10.1186/1471-2105-8-25, 2007

Sutton, M. A., Nemitz, E., Erisman, J. W., Beier, C., Butterbach-Bahl, K., Cellier, P., de Vries, W., Cotrufo, F., Skiba, U., Di Marco, C., Jones, S., Laville, P., Soussana, J. F., Loubet, B., Twigg, M., Famulari, D., Whitehead, J., Gallagher, M. W., Neftel, A., Flechard, C. R., Herrmann, B., Calanca, P. L., Schjoerring, J. K., Daemmgen, U., Horvath, L., Tang, Y. S., Emmett B. A., Tietema A., Peñuelas, J., Kesik M., Brueggemann, N., Pilegaard K., Vesala, T., Campbell, C. L., Olesen, J. E., Dragosits, U., Theobald, M. R., Levy, P., Mobbs, D. C., Milne, R., Viovy, N., Vuichard, N., Smith, J. U., Smith, P., Bergamaschi, P., Fowler, D., and Reis, S.: Challenges in quantifying biosphere–atmosphere exchange of nitrogen species, Environ. Pollut., 150(1), 125–139, https://doi.org/10.1016/j.envpol.2007.04.014, 2007

Teepe, R., Brumme, R., and Beese, F.: Nitrous oxide emissions from soil during freezing and thawing periods, Soil Biol. Biochem., 33(9), 1269–1275, https://doi.org/10.1016/S0038-0717(01)00084-0, 2001

Thompson, R. L., Lassaletta, L., Patra, P. K., Wilson, C., Wells, K. C., Gressent, A., Koffi, E. N., Chipperfield, M. P., Winiwarter, W., Davidson, E. A., Tian, H., and Canadell, J. G.: Acceleration of global N_2O emissions seen from two decades of atmospheric inversion, Nat. Clim. Chang., 9(12), 993–998, https://doi.org/10.1038/s41558-019-0613-7, 2019

Tian, H., Yang, J., Lu, C., Xu, R., Canadell, J. G., Jackson, R. B., Arneth, A., Chang, J., Chen, G., Ciais, P., Gerber, S., Ito, A., Huang, Y., Joos, F., Lienert, S., Messina, P., Olin, S., Pan, S., Peng, C., … Zhu, Q.: The global N_2O model intercomparison project, Bull. Am. Meteorol. Soc., 99(6), 1231–1251, https://doi.org/10.1175/BAMS-D-17-0212.1, 2018

Tian, H., Xu, R., Canadell, J. G., Thompson, R. L., Winiwarter, W., Suntharalingam, P., Davidson, E. A., Ciais, P., Jackson, R. B., Janssens-Maenhout, G., Prather, M. J., Regnier, P., Pan, N., Pan, S., Peters, G. P., Shi, H., Tubiello, F. N., Zaehle, S., Zhou, F., … Yao, Y.: A comprehensive quantification of global nitrous oxide sources and sinks, Nature, 586(7828), 248–256, https://doi.org/10.1038/s41586-020-2780-0, 2020

Van Rossum, G., and Drake Jr, F. L.: Python tutorial, 620, Centrum voor Wiskunde en Informatica, Amsterdam, The Netherlands, 1995

Velthof, G. L., Groenigen, J. W., Gebauer, G., Pietrzak, S., Jarvis, S. C., Pinto, M., Corré, W., and Oenema, O.: Temporal stability of spatial patterns of nitrous oxide fluxes from sloping grassland, J. Environ. Qual., 29(5), 1397–1407, https://doi.org/10.2134/jeq2000.00472425002900050005x, 2000

Wagner-Riddle, C., Congreves, K. A., Abalos, D., Berg, A. A., Brown, S. E., Ambadan, J. T., Gao, X., and Tenuta, M.: Globally important nitrous oxide emissions from croplands induced by freeze–thaw cycles, Nat. Geosci., 10(4), 279–283, https://doi.org/10.1038/ngeo2907, 2017

Walczak, R., Rovdan, E., and Witkowska-Walczak, B.: Water retention characteristics of peat and sand mixtures, Int. Agrophys., 16(2), 2002

Wang, Q., Zhou, F., Shang, Z., Ciais, P., Winiwarter, W., Jackson, R. B., Tubiello, F. N., Janssens-Maenhout, G., Tian, H., Cui, X., Canadell, J. G., Piao, S., and Tao, S.: Data-driven estimates of global nitrous oxide emissions from croplands, Natl. Sci. Rev., 7(2), 441–452, https://doi.org/10.1093/nsr/nwz087, 2020

Wang, C., Amon, B., Schulz, K., and Mehdi, B.: Factors that influence nitrous oxide emissions from agricultural soils as well as their representation in simulation models: A Review, Agronomy, 11(4), 770, https://doi.org/10.3390/agronomy11040770, 2021

Wang, X., Wang, S., Yang, Y., Tian, H., Jetten, M. S. M., Song, C., and Zhu, G.: Hot moment of N_2O emissions in seasonally frozen peatlands, J. ISME, 1(1), 1–11, https://doi.org/10.1038/s41396-023-01389-x, 2023

Wrage, N., Velthof, G. L., Beusichem, M. L. van, and Oenema, O.: Role of nitrifier denitrification in the production of nitrous oxide, Soil Biol. Biochem., 33(12-13), 1723–1732, https://doi.org/10.1016/S0038-0717(01)00096-7, 2001

Wrage-Mönnig, N., Horn, M. A., Well, R., Müller, C., Velthof, G., and Oenema, O.: The role of nitrifier denitrification in the production of nitrous oxide revisited, Soil Biol. Biochem., 33(12–13), 1723–1732, https://doi.org/10.1016/j.soilbio.2018.03.020, 2018

Yanai, J., Sawamoto, T., Oe, T., Kusa, K., Yamakawa, K., Sakamoto, K., Naganawa, T., Inubushi, K., Hatano, R., and Kosaki, T.: Spatial variability of nitrous oxide emissions and their soil-related determining factors in an agricultural field, J. Environ. Qual., 32(6), 1965–1977, https://doi.org/10.2134/jeq2003.1965, 2003

Zeileis, A., Hothorn, T., and Hornik, K.: Model-Based Recursive Partitioning, J. Comput. Graph. Stat., 17(2), 492–514, https://doi.org/10.1198/106186008X319331, 2008

Zhu, X., Burger, M., Doane, T. A., and Horwath, W. R.: Ammonia oxidation pathways and nitrifier denitrification are significant sources of N_2O and NO under low oxygen availability, Proc. Natl. Acad. Sci. U.S.A., 110(16), 6328–6333, https://doi.org/10.1073/pnas.1219993110, 2013